Pergamon

0301-9322(94)E0009-8

Int. J. Multiphase Flow Vol. 20, Suppl., pp. 297–330, 1994
Elsevier Science Ltd
Printed in Great Britain

EXPERIMENTAL METHODS IN FLUIDIZATION RESEARCH

J. G. YATES and S. J. R. SIMONS

Department of Chemical and Biochemical Engineering, University College London, Torrington Place, London WC1E 7JE, England

(Received 3 February 1994)

Abstract—Methods developed over the last 50 years for the investigation of the flow of gases and solids in fluidized suspensions are reviewed. The early use of immersed probes of various kinds is assessed critically and compared with more recently developed non-invasive techniques, such as tomographic imaging. The complete velocity spectrum from bubbling through turbulent to fast operation is considered and the main conclusions obtained regarding gas and particle dynamics are presented.

Key Words: bubbles, circulating beds, FCC, fluidization, hydrodynamics, imaging, tomography

1. INTRODUCTION

Fluidization first became a major industrial unit operation with the introduction of the fluidized catalytic cracking (FCC) process in the early 1940s. The fluidization of solid particles by suspending them in an upward flowing stream of gas had been applied earlier, notably by Winkler in the gasification of lignite and by Godel in the Ignifluid coal combustion process, but it was the success of FCC technology that provided the impetus that led to the proliferation of the technique throughout the modern chemical process industry, and as a result an enormous amount of research work has been carried out into fluidization and its allied subjects during the succeeding 50 years. Much of the early work was concerned with exploring the fluidization characteristics of fine particles with mean diameters of the order of 70–100 μm, such as are used in the FCC process; later, studies were extended to coarser materials such as sand and glass ballotini.

One of the first generalizations to come from this empirical work was the so-called "two-phase" theory of Toomey & Johnstone (1952), which proposed that once the velocity of a gas flowing through a bed of powder exceeded the minimum necessary to just fluidize it, then any excess flow passed through in the form of gas bubbles which were thought to behave in a similar manner to air bubbles rising through a column of water. Bubbles had been a familiar feature of fluidized beds from the earliest studies and it soon became apparent that they were responsible for many of the advantages and disadvantages of fluid bed operation. The high degree of mixing of the bed solids was found to be the result of the vertical movement of particles carried in the wake region behind bubbles and this gave rise to the excellent heat transfer properties of the bed. On the other hand, gas flowing inside bubbles was found to have little contact with the bed solids and this by-passing effect in some cases severely limited the extent of the gas–solid reaction that could be achieved.

The first satisfactory theory of bubble motion in fluidized beds was proposed by Davidson (1961) and was later developed by Davidson & Harrison (1963), Jackson (1963a, b), Murray (1965a, b) and others. The Davidson theory has been described as "the seminal concept that guided research and advanced understanding of dense bubbling fluidized beds" (Kunii & Levenspiel 1991) and it led to the development of many diverse experimental techniques which were designed to probe the properties and behaviour of bubbles and to study the effects resulting from their flow. Some of these diagnostic techniques will be described below.

A second generalization of considerable utility was introduced by Geldart (1973), in which he separated fluidized powders into four groups A, B, C and D according to the size and density of their component particles. Group A powders were those like the FCC catalyst, which showed a degree of uniform expansion between the minimum fluidization velocity, U_{mf}, and a higher velocity,

minimum bubbling velocity, U_{mb}, at which bubbles first appeared; group B powders, such as coarse sand, formed bubbles as soon as U_{mf} was exceeded. Powders in group C were light and very finely divided and were often difficult to fluidize in the normal way; they are cohesive materials such as talc, flour and cement. Group D were large and dense and prone to spouting rather than fluidizing. As with the Davidson theory, the Geldart classification has spawned a great deal of experimental and theoretical work involving many different techniques and it is still the cause of heated debate, particularly among theoreticians.

In recent years, largely as a result of a growing interest in fluidized bed combustion and gasification processes, much attention has been paid to beds operated at high gas velocities and low solids loadings, conditions which give rise to strong entrainment and elutriation of solids and require them to be recycled in a circulating loop. New experimental methods have had to be devised to study these circulating systems.

The review that follows will consider the main experimental techniques that have been developed to investigate gas-fluidized beds across the velocity spectrum from the low-velocity bubbling systems through turbulent to fast circulating beds. Methods for studying the dynamics of the gas phase in both bubbling and circulating beds will be described, as well as those designed to follow and account for the motion of bed particles.

2. METHODS FOR STUDYING GAS DYNAMICS

The flow of gas, whether in the form of bubbles or emulsion, is one of the most important factors determining the behaviour of a fluidized bed. Bubbles are not directly observable in large-scale industrial units and even on the laboratory scale the use of tubular glass-walled vessels only allows those bubbles that travel up the vessel wall to be seen. If, however, the containing vessel is constructed from two flat parallel-sided transparent plates separated by a small distance, say 1 cm, bubbles rising through the bed of powder rapidly become big enough through coalescence to span the distance between the plates and they are then visible to the naked eye. This is called a "two-dimensional", or 2-D, fluidized bed and, in effect, it represents a vertical slice through a truly 3-D system. Ciné photography or video imaging may be used to record the flow of bubble gas and the images obtained may be analysed either on- or off-line to give quantitative information on bubble flow, coalescence etc. Many of the earlier academic studies on fluidization were carried out using these 2-D systems and they provided a great deal of insight into the behaviour of bubbling beds (Rowe 1971).

A recent application of such a system was described by Hailu *et al.* (1993), who set out to measure the throughflow velocity of gas inside a rising bubble. The throughflow velocity is predicted by a number of the theories referred to above to be in excess of the minimum fluidization velocity, U_{mf}; thus, Davidson & Harrison (1963) showed that the gas velocity across any plane through the bubble normal to the vertical axis is 2 U_{mf} for a 2-D bubble and 3 U_{mf} for a 3-D bubble. Hailu *et al.* (1993) injected single bubbles containing very small and light tracer particles into an incipiently fluidized 2-D bed of coarse sand and used laser-Doppler velocimetry to observe the circulation of the tracer particles induced by the gas throughflow inside the bubbles. They concluded that the throughflow velocity ranges from 0.8 U_{mf} in the middle of the bed, in agreement with the model of Murray (1965b), to 1.8 U_{mf} near the bed surface, as predicted by Davidson & Harrison (1963).

Despite their usefulness there is always some doubt as to whether the behaviour observed in 2-D beds can be directly extrapolated to three dimensions and, as a result, a number of other methods have been developed to investigate gas flow in realistic units. Several of these methods involve the use of sensors of various kinds either immersed in the bed or located in the bed walls and these will now be described in detail.

2.1. Probes and Sensors

2.1.1. Optical sensors

One of the earliest reports of the use of optical sensors was that by Yasui & Johanson (1958) and the methodology they adopted has formed the basis of many subsequent studies. They used a light source consisting of a 3.175 mm dia tungsten filament lamp coupled to a 2.38 mm o.d. metal

tube; facing the lamp was a small mirrored glass prism cemented to one end of a 4 mm dia clear quartz tube which was wrapped with aluminium foil. Two such probes separated by a short variable distance were positioned one above the other and the assembly was immersed in a fluidized bed of powder. When a bubble filled the space between the lamp and the prism, light was transmitted to the prism and reflected out through the quartz rod into a vacuum phototube. Here the light pulse was converted into an electrical signal which was amplified and recorded on the moving chart of an oscillograph. The bubble rise velocity was estimated from the time lag between the signals from the two probes and from their known distance apart. The system was not able to provide information on bubble volumes but the results clearly showed that bubbles increase in size and velocity as they rise up in the bed; increases in the particle size of the bed material and increase in fluidizing gas velocity were also shown to increase the bubble velocity.

A device based on the same principles as that of Yasui and Johanson, but consisting of a 14 × 14 array of probes covering an area of 0.68 m^2 was described by Whitehead & Young (1967). This was immersed to varying depths in a 1.2 m^2 bed of sand and used to analyse bed behaviour and bubble properties over a wide range of operating conditions. Although the scale of scrutiny of individual probes was quite coarse, the array did give useful information on the behaviour of large beds and, particularly, on the formation and location of preferred bubble tracks within the bed.

Put *et al.* (1973) used a single light source situated a variable distance opposite a photodiode detector to monitor bubble flow in a freely bubbling bed. The number of bubbles passing through the probe was counted over a period of 21 min and from the known distance of separation of the source and detector the cumulative density function of bubble width was obtained. The results were in substantial agreement with those of Yasui & Johanson (1958) referred to above.

A small optical fibre probe developed by Okhi & Shirai (1976) consisted of three fibres bound together such that the fibre at the centre of the bundle provided the illumination that was detected by the other two. The probe was designed primarily to study the movement of solid particles in a bed but it was adapted to investigate bubble flow. The illuminating and detecting fibres were bent in the form of a horseshoe with a gap of 5 mm between them (figure 1). Light from a stroboscope of known flash frequency was sent down the illuminating fibre and the detected light passed to a photomultiplier. The local bubble fraction was then found by dividing the mean frequency of the photomultiplier output signal by the stroboscope flash frequency.

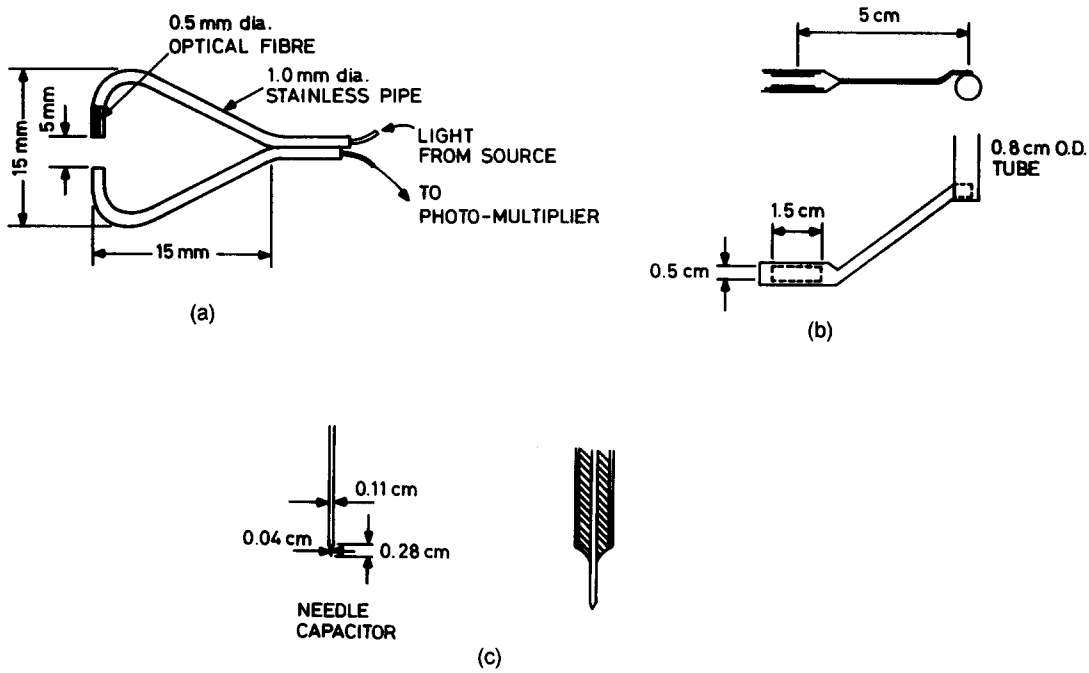

Figure 1. Some probes used in fluidized beds: (a) optical probe (Okhi & Shirai 1976); (b) capacitance probe (Geldart & Kelsey 1972); (c) needle capacitance probe (Werther & Molerus 1973a).

Yoshida *et al.* (1978) used laser light passing through a horizontal steel pipe of 6 mm dia to illuminate an optical fibre located inside a similar pipe introduced from the opposite side of the bed. Light from the fibre fell onto a phototransistor, the current from which was amplified and recorded on an oscillograph. The horizontal distance between the light source and the fibre tip was adjustable, as was the vertical position of the probe in the bed. Measurements were made of the size distribution of bubbles at positions from close to the distributor to the bed surface; the distributions were found to be bi-modal, a result in contrast to those of other workers using less invasive techniques of observation (Rowe & Yacono 1976).

Light sensors, in general, have not proved as effective as other techniques for measuring local properties of bubbling fluidized beds. One obvious source of uncertainty is the extent to which some of the probes interfere with the flow of gas and bubbles [see below under Rowe & Masson (1981)]; the interpretation of the electrical signals generated by the probes is another potential source of problems. Optical probes have, however, been applied with greater success in the study of the movement of solid particles, particularly in high-velocity circulating beds; these applications will be considered below.

2.1.2. Capacitance sensors

The principle here is that the capacitance of a gas–solid mixture, such as the emulsion phase of a fluidized bed, is a strong function of the concentration of solids in the mixture. A probe inserted into a bed to measure a local value of capacitance will thus respond to a change in the local solids concentration, such as occurs when a gas bubble engulfs the probe. Fluidized bed particles are typically electrical insulators (silica, cracking catalyst etc.) and hence capacitance is a more appropriate property to measure than electrical resistance or conductivity, although such properties have been investigated from time to time (Park *et al.* 1969).

Morse & Ballou (1951) were amongst the first to report the used of a capacitance probe to investigate the "uniformity of fluidization" of a bed of fine particles, although their results were largely qualitative. Lanneau (1960) used the same technique to obtain more comprehensive data on the performance of a bed of microspherical alumina particles with a mean diameter of about 80 μm. The bed container was a tubular vessel of 7.5 cm dia and some 10 m in height; the powder bed itself was 5 m deep and probes or pressure tappings could be inserted at 15 cm intervals along the entire length. The probes were parallel-plate condensers connected to an oscillator and then to a oscillograph; they were inserted horizontally so that the probe tips were at the centre of the bed. The probe calibration procedure was not described but Lanneau stated that its response was linear for changes in the solids concentration at the tip. Tests were carried out at varying gas velocities and pressures and from the probe responses a number of conclusions were drawn regarding bed behaviour. Thus, at low gas velocities the bed has a two-phase structure with well-formed bubbles containing few solids. At higher velocities the bubbles began to break up into smaller units containing a higher proportion of solids, while at the highest velocities (1–2 m/s) a condition of uniform "particulate" fluidization was achieved. There is some doubt over the validity of Lanneau's conclusions, particularly in the absence of any details about probe calibration and the fact that a bed with such a high aspect ratio was almost certainly operating in the slugging mode over much of the range of gas velocities used.

The problems inherent in interpreting the results of capacitance probe measurements were discussed at length by Geldart & Kelsey (1972). Their capacitance probe head was of a similar design to that of Lanneau and consisted of two parallel rectangular plates 1.5 × 0.5 cm separated by a gap of 0.5 cm (figure 1). The head was attached to the end of a 0.8 cm dia tube, which carried the necessary cables to the electrical circuit. This consisted of a tunable oscillator with a natural frequency of 2 MHz, but which varied according to the concentration of particles between the plates. These variations were converted by a discriminator into changes in d.c. voltage and the signal was amplified and recorded by a UV oscillograph. The probe was first tested in a 2-D bed of fluidized sand and its response compared to the direct observations made by ciné filming the bed at 64 frame/s. The first tests, in which the probe head was mounted close to the end of the support tube, showed clearly that the rising bubbles were considerably distorted by the probe and in many cases were split into two. This problem was largely overcome by displacing the head from the tube, as shown in figure 1, but there was still uncertainty as to whether the probe was responding

to bubble voids or to regions of reduced solids concentration around the voids. For calibration the probe was lowered into a bed of sand held at the point of incipient fluidization and the maximum signal displacement between voidage $\varepsilon = 1.0$ and $\varepsilon = \varepsilon_{mf}$ was measured. The film record of the probe in a gently bubbling 2-D bed showed that signal peak heights greater than half the maximum then corresponded to bubbles that enveloped at least half the probe. When applied to a 3-D bed it was found necessary first to calibrate the probe by comparing its readings with film taken of the bed surface at which bubbles were bursting. Agreement between the two was not good, particularly at low gas flow rates where bubbles are small. Geldart & Kelsey (1972) concluded that capacitance probes to be used in a 3-D bed should be calibrated *in situ*, preferably using a non-invasive technique such as X-ray ciné photography and, furthermore, that results obtained from systems not carefully calibrated may be in error by up to a factor of 10. A somewhat similar but more detailed investigation of the observation of bubble–probe interaction by ciné photography was reported by Gunn & Al Doori (1985). They also stressed the importance of proper calibration of the probe and of allowing for the stochastic interaction between the bubble interface and the probe.

Werther & Molerus (1973a, b) carried out a meticulous study on the design and use of capacitance probes that has been the touchstone for subsequent work in this area. They set out to determine local values of bubble gas flow, bubble volume fraction, mean pierced bubble length and mean bubble rise velocity and identified the essential features of a probe suitable for the purpose. Such a probe should:

(i) disturb the bed as little as possible;
(ii) measure local variations;
(iii) have a rapid response to changes in voidage;
(iv) have adequate mechanical strength;
(v) be moveable within the bed;
(vi) be compatible with the bed solids.

These considerations led to the development of a miniature capacitance probe shaped in the form of a spike with a central protruding needle forming one pole and the enclosing metal tube the other pole of the capacitor (figure 1). Initial tests were carried out to determine the extent to which the probe interfered with the flow of gas through a bed and it was concluded that there was minimal interference. The probe was connected via an oscillator to a reactance converter, a discriminator circuit and finally to a correlator (figure 2). The discriminator was necessary in order to decouple the effects on the output signal, U_t, of the bubble phase and local variations in the voidage of the emulsion phase. It was expected that the signal pulses due to bubbles would be significantly the stronger of the two and that a separation of the two parts of the signal could be achieved by a simple limiting technique, somewhat along the lines of the procedure adopted by Geldart & Kelsey (1972). The method is shown in figure 2, where that part of the signal that lies below an adjustable reference value is transmitted and the rest is held at a constant value U_D. The transmitted pulses were then converted into rectangular shapes of constant height $U''(t)$, the duration of which, t_G, is equal to the time during which the probe sees a bubble. The shape of the signal produced when the probe is hit by a bubble is shown in figure 3, from which it may be seen that t_G is equal to the duration, t_b, of the corresponding bubble pulse only if the discriminator cuts the bubble pulse at half its height. This will not normally be the case and so it was necessary to derive a more general relationship between t_G and t_b as follows:

$$t_b = t_G + t_r\left[2\left(\frac{U_1 - U_D}{E[z]}\right) - 1\right], \qquad [1]$$

where t_r is the mean time of rise of a trapezoidal pulse [i.e. $(t_2 - t_1)$ or $(t_3 - t_4)$ in figure 4], $E[z]$ is the mean height of the bubble pulses and U_1 is the mean value of the signal component due to changes in the emulsion phase voidage. The pierced length, l_b, of a bubble is related to the local mean bubble rise velocity, v_b, by

$$l_b = v_b t_b. \qquad [2]$$

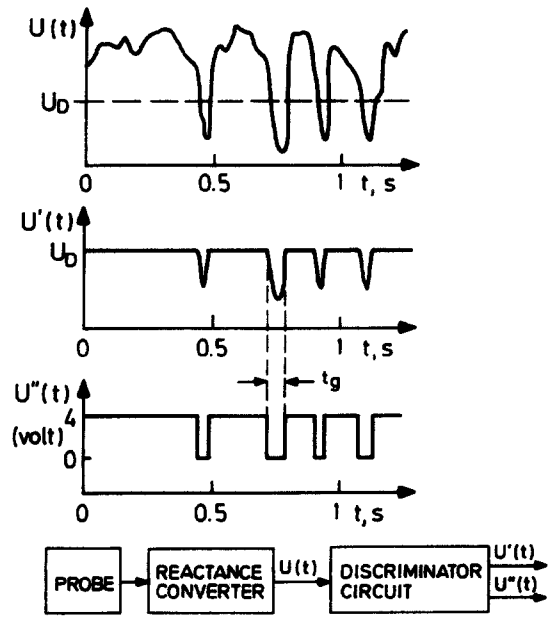

Figure 2. Processing of the capacitance probe signal (Werther & Molerus, 1973a).

The mean bubble velocity at any point in the fluidized bed was found by using two capacitance probes joined together with the tip of one separated from that of the other by distances, s, from 0.4 to 2 cm.

Now the cross-correlation function between two continuous stationary and random ergodic variables is given by

$$\phi_{AB}(\tau) = \lim_{T\to\infty} \frac{1}{2T} \int_{-T}^{+T} U'_A(t) U'_B(t+\tau) \mathrm{d}t, \qquad [3]$$

where $U'_A(t)$ is the value of the first variable sampled at time (t) and $U'_B(t+\tau)$ is the value of the second variable sampled at time $(t+\tau)$. The signals from the two probes were cross-correlated on the basis of [3] by the correlator built into the circuit and from the maximum on the plot of cross-correlation function against time the mean time $E[t_a]$ for the bubbles to rise the distance s was found. Then,

$$v_b = \frac{s}{E[t_a]}. \qquad [4]$$

The mean number of bubbles per unit time striking a probe was also determined and used in combination with v_b and t_b to derive further characteristics of the local state of fluidization, such as the radial distribution of bubble flow (figure 4).

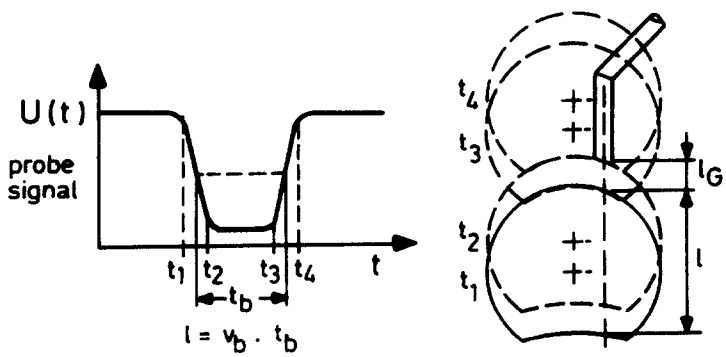

Figure 3. Probe signal when the capacitance probe is hit by a rising bubble (Werther & Molerus 1973a).

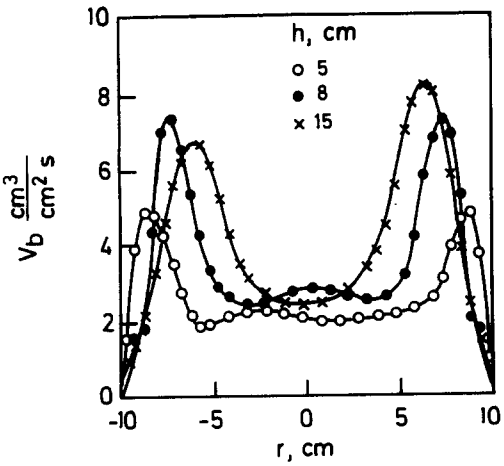

Figure 4. Variation of the local bubble gas flow with radial displacement of the probe from the vessel centreline for different heights, h, above the distributor (quartz sand of mean particle size 83 μm fluidized by air in a 20 cm dia bed at a gas velocity of 9 cm/s) (Werther & Molerus 1973a).

2.1.3. Pressure sensors

Pressure measurements have always been used in work on fluidized beds. Measurement of the overall bed pressure drop as a function of the velocity of the gas flow through the bed is used to determine the minimum fluidization velocity of the bed material. Also, time-averaged values of the pressure difference between different locations are used routinely on industrial units to give an indication of bed height.

More detailed information on system hydrodynamics is, however, available from the study of pressure fluctuations within the bed. These fluctuations are generally acknowledged to be due to the flow of bubbles, but the exact details of cause and effect have been the source of much discussion. The eruption of bubbles at the bed surface could cause pressure waves to travel back down the bed, as could the coalescence of bubbles below the bed surface; bubble formation at the distributor is also thought to lead to pressure variations. One of the earliest studies of these phenomena was that of Winter (1968), who used an electrical conductivity cell to record pressure variations with time; the radial centre of the bed was connected to the cell through a 7 mm dia glass tube, a change in pressure causing a change in the liquid level in the cell which directly affected the resistance of a platinum electrode; the resulting electrical signal was amplified and recorded. The pressure fluctuations were recorded over a period of 6 s at several locations and a statistical analysis was applied to the results. Bed densities were recorded simultaneously using both a light probe and a radioactive source and it was concluded that in beds of small particles and at low gas velocities the density distributions and the intensity of pressure fluctuations were strongly asymmetric, but that they became normally distributed at higher velocities.

Taylor *et al.* (1973) used a pressure transducer fitted at different positions in the container wall of beds of glass ballotini and showed that the frequency of the recorded pressure fluctuations varied with bed depth (figure 5). The spectral power density of the recorded signals was computed and used as a measure of the "quality" of fluidization under various operating conditions.

Correlation analysis of pressure signals from two transducers exposed to a bubbling bed was discussed first by Swinehart (1966) and later by Kang *et al.* (1967), Lirag & Littman (1971) and by Sitnai (1982). The technique was developed for on-line analysis by Fan *et al.* (1981). These workers used a correlation and probability analyser to determine the auto- and cross-correlation functions, the probability density function and the probability distribution function of the fluctuating signal from a differential pressure transducer situated in the wall of the bed container. These are shown in figures 6 and 7 and they were used by Fan *et al.* to investigate the causes of the pressure variations. Thus, cross-correlation of the signals from two tapping points close to the bed surface and separated by a distance of 10 cm (figure 7) showed that the upper tap had a time delay of 0.101 s compared to the signal from the lower tap. If the pressure fluctuations had been caused by fluctuations in the bed surface caused by bubble eruption, as suggested by Lirag &

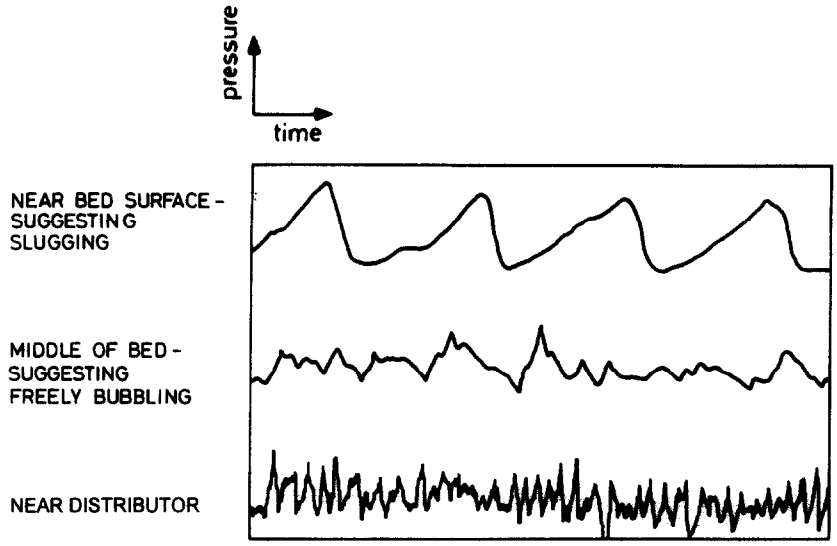

Figure 5. Pressure fluctuations along the height of a fluidized bed of cracking catalyst (Cheremissinoff 1986).

Littman (1971), then the upper tap would have responded in advance of the lower but this was not the case. The authors therefore conclude that the signals are caused by single large bubbles rising between the tappings. Previous work (Littman & Homolka 1970) had shown that when a single bubble passes a pressure sensor a pressure peak is registered as the bubble roof touches the tap and a pressure trough as the bubble floor reaches it. These peaks and troughs would therefore appear to be the cause of the fluctuations recorded sequentially by the two tappings of Fan *et al.* (1981).

In a second report from the same group (Fan *et al.* 1983), the measurements were extended to higher gas velocities so that the beds of particles passed from the bubbling to the slugging and finally to the turbulent regime. Cross-correlation based on the equivalent of [3] and [4] was used to determine the velocity of the fluctuation waveforms which were equated to the velocities of bubbles and slugs in the first two regimes. It was shown that these velocities increase as fluidizing velocity increases (figure 8) up to the point at which turbulent flow is established when the waveform velocity becomes essentially constant. This diagnostic test has been used by other workers to establish the onset of turbulent flow (see below).

Geldart & Xie (1992) recently reported work on the use of pressure sensors immersed in beds of group A powders. Owing to the small particle size of such materials there is a tendency for the

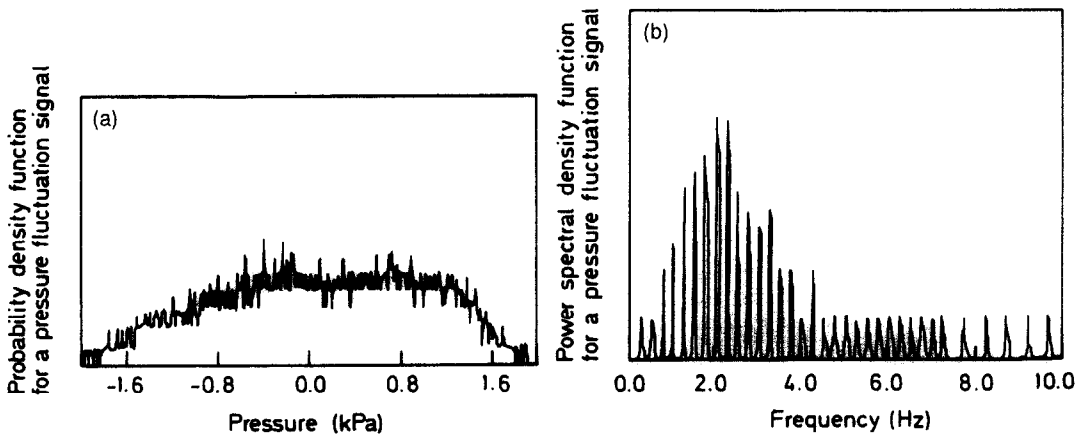

Figure 6. Characteristics of pressure fluctuation signals in fluidized beds: (a) probability density function; (b) power spectral density function (Fan *et al.* 1981).

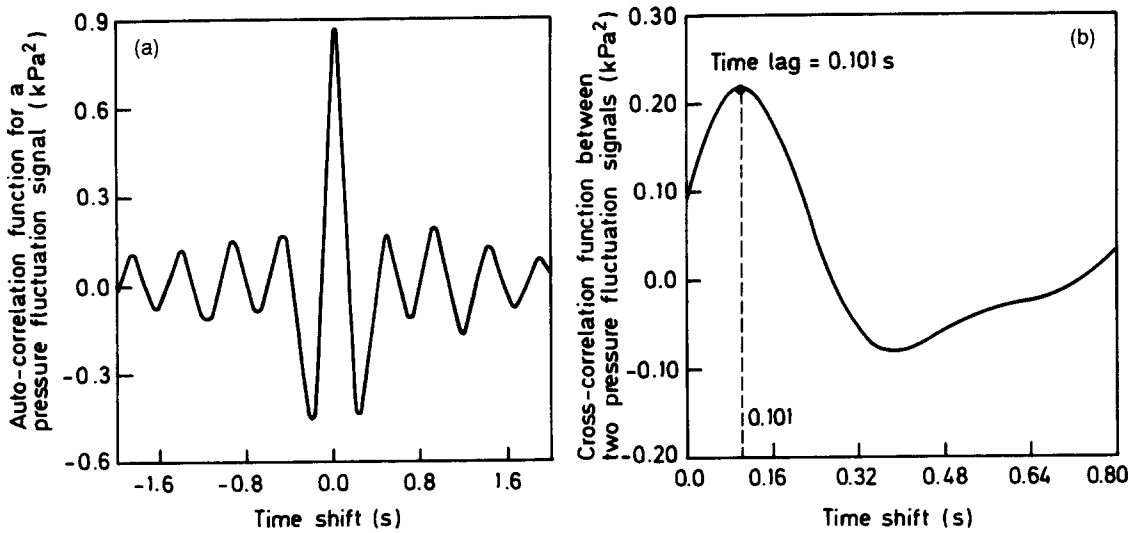

Figure 7. Characteristics of pressure fluctuation signals in fluidized beds: (a) auto-correlation function; (b) cross-correlation function (Fan *et al.* 1981).

probes to become blocked with powder and it is then necessary to purge them with gas. Geldart & Xie (1992) found that the velocity of gas through the end of the probe can be relatively low (0.15 m/s) for coarse group A powders but that it should be as high as 0.5 m/s for finer materials. Furthermore, the stream of small bubbles produced by the purge gas limits the size of bubbles that can be detected to >3 cm.

The effect of temperature on the behaviour of fluidized beds was investigated by Svoboda *et al.* (1983) using pressure sensors and applying statistical analysis to the results. The frequency spectrum, dominant frequency and mean pressure amplitudes measured in beds of corundum, lime and coal ash were found to depend strongly on the operating temperature, the dominant frequency increasing and the amplitude of fluctuations decreasing as the temperature was raised from ambient to 800°C. These observations were consistent with an improvement in the "quality" of fluidization, smaller bubbles being more prevalent and larger bubbles less stable at the higher temperatures.

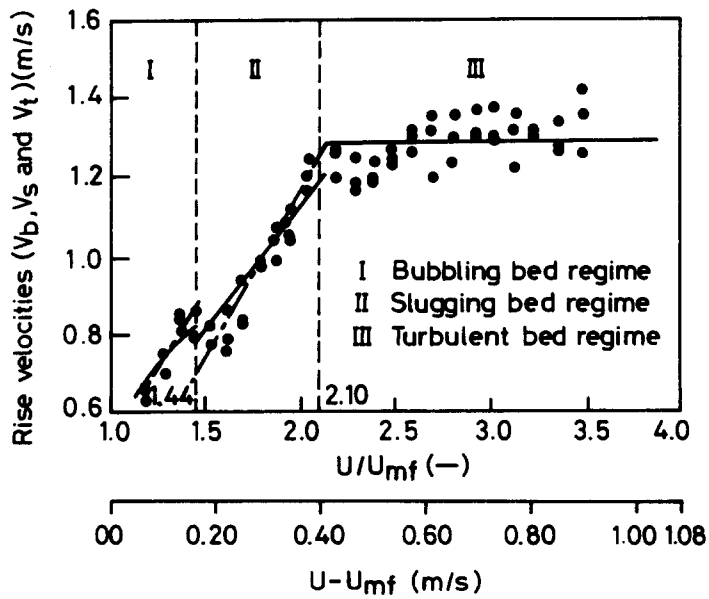

Figure 8. Rise velocities of bubbles, slugs and pressure waves as a function of dimensionless air flow rate (Fan *et al.* 1983).

An unusual application of the use of pressure sensors was described by Roy *et al.* (1990), who used them to measure the velocity of sound in a fluidized bed. The velocity of sound, u_s, in a fluid is given by

$$u_s = \sqrt{\frac{\kappa}{\rho}}, \qquad [5]$$

where κ is the bulk modulus of elasticity and ρ is the density of the fluid. Roy *et al.* (1990) argued that in a gas–solid fluidized bed the relevant elasticity is that of the gas, whereas the relevant density is that of the particle bed which is often 1000 times that of the gas. In a bed of solids fluidized by air, therefore, the velocity of sound should be $1/(1000)^{1/2}$ times the velocity of sound in air, 300 m/s, i.e. about 10 m/s. The authors give a more rigorous derivation, starting with an expression for the velocity of a plane wave in a continuous compressible medium:

$$u_s = \sqrt{\frac{dp}{d\rho}}, \qquad [6]$$

where p is the pressure and ρ is the bulk density. The following assumptions are then made for a fluidized bed of particles:

(i) the relative motion between gas and particles is negligible;
(ii) the interstitial gas is compressible and obeys the ideal gas law;
(iii) the bed responds isothermally to the passage of a compression wave;
(iv) the particles are incompressible.

On this basis, an expression for the velocity of sound is obtained:

$$u_s = u_{s0}\sqrt{\frac{\rho_g}{\gamma\varepsilon[\rho_s(1-\varepsilon)+\rho_g\varepsilon]}}, \qquad [7]$$

where u_{s0} is the velocity of sound in the gas, γ is the ratio of the specific heats of the gas, ρ_s is the solids density and ε is the voidage of the bed. Again, for an air fluidized bed of sand particles, u_s turns out to be about 10 m/s. Experiments were carried out in which a tall bed of particles was incipiently fluidized by a supply of air at its base (figure 9). A secondary source of air was admitted further up through a side tube at such a velocity as to cause vigorous bubbling or slugging above the tube. Two pressure probes situated in the incipiently fluidized zone recorded pressure fluctuations originating from the upper bubbling region and these were cross-correlated to give the time delay between the signals and from the known separation of the probes the velocity of propagation of the pressure pulse was obtained. Roy *et al.* (1990) used beds of several materials of different size and density and found in all cases good agreement between the measured velocities and those u_s values calculated from [7]. They also point out in their conclusions that measured u_s values could be used to obtain values of the solids density, ρ_s, a quantity that can be difficult to measure, particularly in the case of porous solids.

Theories relating to the stability of fluidized beds have been the source of much controversy in recent years and a number of studies of pressure fluctuations have been carried out in order to provide supporting evidence for one theory or another. The stability criterion first proposed by Wallis (1969), and more recently explored by Foscolo & Gibilaro (1984) and co-workers, is based on the "two-fluid" model, which considers a fluidized bed to be made up of two interpenetrating incompressible continua, the gas phase itself and the particle phase which is assumed to behave as a fluid under the influence of the gas–particle interaction forces. On the basis of the model (Foscolo & Gibilaro 1984; Gibilaro 1994), it can be shown that disturbances within a bed propagate in the form of either dynamic or continuity waves, the velocities of which are, respectively:

$$u_e = \sqrt{\frac{3.2gd_p(1-\varepsilon)(\rho_p-\rho_f)}{\rho_p}} \qquad [8]$$

and

$$u_c = nu_t(1-\varepsilon)\varepsilon^{n-1}, \qquad [9]$$

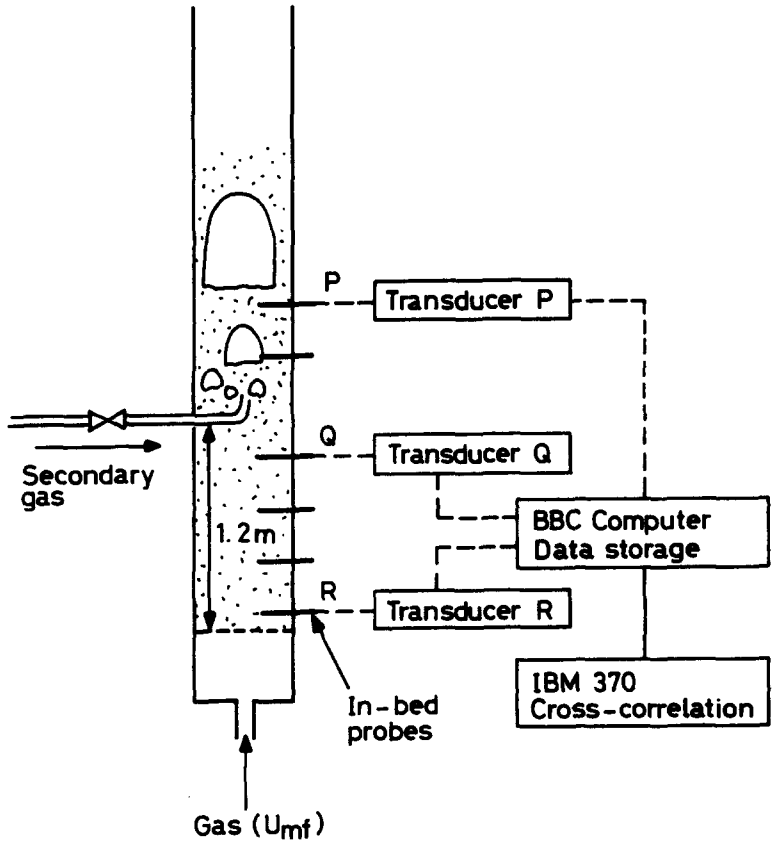

Figure 9. Apparatus to give a slugging fluidized bed above an incipiently fluidized bed (Roy *et al.* 1990).

where d_p is the particle diameter, ρ_p and ρ_f are the particle and fluid densities, respectively, u_t is the terminal fall velocity of a single particle and n is the index in the Richardson–Zaki equation. The stability limit occurs when

$$u_e = u_\varepsilon. \qquad [10]$$

If the velocity of the dynamic wave exceeds that of the continuity wave then bubbles cannot form and the bed will expand uniformly with increasing fluid velocity, a type of behaviour associated with liquid–solid fluidization. If the reverse is true then bubbles form. The bubbling criterion may be formulated as follows:

$$\left[\frac{gd_p(\rho_p-\rho_f)}{u_t^2\rho_p}\right]^{0.5} - 0.56n(1-\varepsilon)^{0.5}\varepsilon^{n-1} = \left\{\begin{array}{c}+\text{ve,stable}\\ -\text{ve,unstable}\end{array}\right\}. \qquad [11]$$

If the left-hand side is zero this will be the point of minimum bubbling and the voidage will be the minimum bubbling voidage, ε_{mb}.

Gibilaro *et al.* (1988) connected a differential pressure transducer to a bed of copper particles fluidized by water and determined the statistics of the pressure fluctuations registered as the flow of water was increased. They found that root-mean-square values of the pressure signals increased sharply as the transition was made from stable to unstable behaviour, i.e. from non-bubbling to bubbling, and that the transition point was as predicted by the criterion given in [11].

The Foscolo–Gibilaro criterion has recently been studied in gas fluidized beds by Musmarra *et al.* (1992) using pressure measurements in a system somewhat similar to that used by Roy *et al.* (1990). Musmarra *et al.* find good agreement between their measurements of pressure propagation velocity and that given by [5] but observe that the dynamic wave velocity given by [8] is 2 orders of magnitude lower than this. Further work is clearly needed in this area.

Before moving on to consider other techniques, it is worth sounding a cautionary note about the use of immersed probes in examining bubble dynamics. A study was carried out by Rowe &

Masson (1981), in which they used X-ray ciné photography to view the interior of a fluidized bed containing a variety of probes of different size and shape. The bed was held just above the point of minimum fluidization and single bubbles were injected in from a nozzle located in the distributor. They concluded that all probes disturb the bubbles to a greater or less extent and that the most common effect is to cause them to accelerate, elongate and deviate so that they climb the probe stem. It is not clear, however, whether the effects would be seen to the same extent in a freely bubbling bed where bubble coalescence is a dominant feature.

2.2. Imaging Techniques

Investigative techniques utilizing the attenuation of a transmitted energy beam to produce an image were applied at an early stage to fluidized systems. Such techniques have the major advantages, when compared to other methods, of being totally non-invasive (there being no internal probes to interfere physically with the process) and insignificantly affected by harsh conditions such as high temperatures and pressures. Whilst the data is normally presented in terms of solids concentration profiles, from which gas phase dynamics can be inferred, some imaging techniques have been applied directly to the measurement of bubble phenomena.

2.2.1. X-ray attenuation

The majority of the work carried out on fluidized systems using X-ray attenuation has been conducted by Rowe, Yates and co-workers at University College London (UCL). Investigations have been centred on the behaviour of gas bubbles in solid beds, phenomena such as bubble growth, bubble splitting (with and without the presence of internal heat exchanger tubes), the effects of gas distribution, elevated temperatures and pressures and co-axial nozzles (amongst others) all being studied via X-ray images. The essential elements of the X-ray equipment are shown in figure 10, although over the years modifications have been made to the original device [described in Rowe & Partridge (1965)], the most significant being the manner in which the images are captured and analysed. Initially, images of the bubbles were projected from ciné film negatives on to a screen and a circle drawn by hand around each bubble to find the bubble diameters. For velocity measurements each bubble was then followed over a few centimetres of travel by measuring the movement of the centre of the fitted circle from a datum line on the photograph. This technique was subsequently improved (Rowe & Yacono 1976) by projecting the images on to the table of a Hewlett Packard 9874A digitizer and tracing the bubble outlines with a hand-held cursor. The digitizer was coupled to a computer which converted the bubble silhouettes from the digitized co-ordinates to population statistics of average bubble diameter, volume, velocity etc. Under a given set of conditions, a sample of at least 200 bubbles was used to estimate these parameters. Not surprisingly, therefore, this method still proved to be an exceedingly laborious and tedious exercise, so recent innovations (Yates & Cheesman 1992) have incorporated an image analysis system, consisting of a JVC video recorder/player and a 386 PC with framestore board on Bioscan Optimas software to control the image capture, manipulation and data extraction. Image storage and colour print-out facilities complete the equipment configuration.

With the enhanced system the X-ray beam is passed horizontally through the bed at a chosen level and images are captured by the video recorder at a rate equivalent to 25 frame/s. The recorder is synchronized with the X-ray source, which produces pulses of energy of 1 ms duration. In a freely bubbling bed there will be a degree of "shadowing" of bubbles in line with the beam but, since the rise velocity of a bubble is a function of its size, two differently sized bubbles will generally separate as they rise through the field of view, thus enabling each to be observed. An example of a computer-processed image of a single bubble rising through a bed of group B powder held at the point of incipient fluidization is shown in figure 11. The different colours represent the X-ray transmitted intensities, which differ as a result of the beam passing through zones of different porosity around the bubble. The black area is the emulsion phase with an average porosity of 0.445, the green with 0.495, the blue with 0.526, the cyan with 0.627 and the red area is the bubble void itself with a porosity of 1.0. Two points must be emphasized. Firstly, the computer is programmed to calculate average values of voidage between any predetermined intensity values and to colour code that range; there is, in fact, a continuous gradation in voidage between one zone and the next.

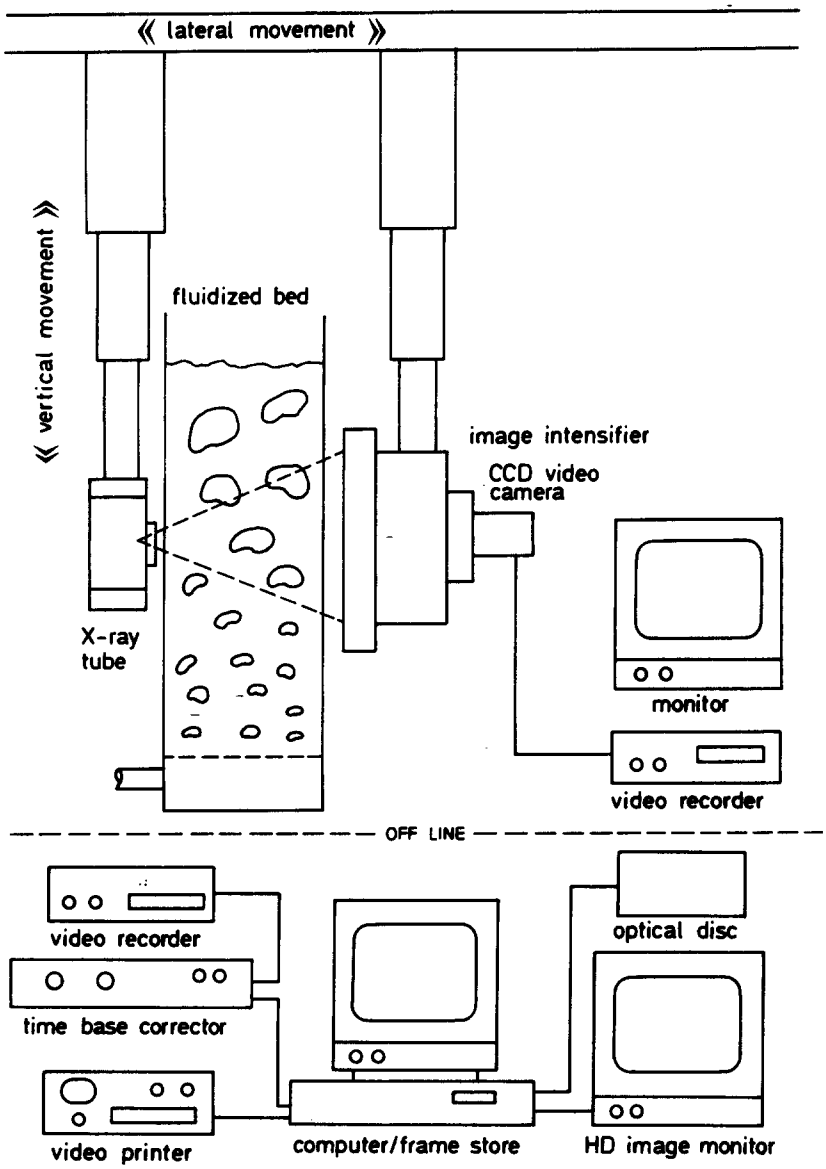

Figure 10. X-Ray attenuation equipment (UCL, London).

Secondly, the image is a representation in two dimensions of a truly 3-D object, a silhouette in other words, and this means that the voidage indicated is an average value across a chord of the more or less spherical region around the bubble. Point values of the voidage may be obtained by deconvolution of the silhouette using the Abel transform (Bracewell 1986), which is based on the assumption that the 3-D object being considered is symmetrical about a vertical axis through its centre; isolated bubbles in fluidized beds have sufficient axial symmetry for the transform to be applicable and the method has been applied recently to obtain both radial and axial profiles of the solids concentration around bubbles in beds of powders in groups A and B (Yates *et al.* 1994). In order to determine fluid bed voidages using X-rays it is first necessary to calibrate the system. When X-rays pass through a material they are attenuated by absorption, reflection and scattering and the extent of the attenuation is a function of the chemical nature of the solid particles and of the quantity of material in the path of the beam. The extent of attenuation is given by the Beer–Lambert relationship:

$$I = I_0 \exp(-\mu c t), \qquad [12]$$

where

I = the transmitted intensity,
I_0 = the incident intensity,
μ = the attenuation coefficient of the material,
c = concentration

and

t = the path length.

Equation [12] may be expanded to

$$I = I_0 - I_0(\mu ct) + \ldots \quad [13]$$

Frequently, the second and higher order terms in the exponential may be neglected and the linear form of [13] is then satisfactory. Since the attenuation of X-rays by ambient air is negligible, the concentration, c, in [13] can be expressed in terms of the solids fraction of the fluidized bed through which the beam passes:

$$I = I_0 - (I_0\mu)(1 - \varepsilon)t, \quad [14]$$

where

ε = the voidage of the bed material.

The system can be calibrated according to [14] by using a wedge-shaped vessel made from a material transparent to X-rays, such as aluminium, and filled with a packed bed of the powder to be studied. The wedge is set up vertically in the X-ray beam and the transmitted intensity measured on a range of grey scales from 0 to 225 as a function of the wedge thickness, t_w. Linear regression of the data gives values for I_0 and the coefficient of t in [14] and from the known value of the packed-bed voidage an explicit relationship between the voidage, transmitted intensity and path length for any sample of the powder may be found (Yates *et al.* 1994).

2.2.2. γ-Ray attenuation

Investigations on laboratory-scale fluidized beds using γ-ray attenuation have been widely reported. Baumgarten & Pigford (1960), Bloore & Botterill (1961) and Clough & Weimer (1985) all studied gas-bubble sizes and frequencies under different operating conditions with density gauge-type devices which could travel vertically up and down the fluidized bed vessels in question. Orcutt & Carpenter (1971) used a similar device to study bubble coalescence. Such gauges measure the ionization of gas in a radiation detector as a function of the amount of radiation received. By calibration, therefore, the output signal is directly related to the voidage between the radiation source and detector. Weimer *et al.* (1985) have conducted a comprehensive investigation on the use of γ-ray attenuation gauges on fluidized bed systems. They used a modified, off-the-shelf, density gauge (500 mCi point source of ^{137}Cs) to measure the two-phase properties of both a 0.292 m dia bed, operating at ambient temperature and pressure, and a 0.128 m dia bed, operating at pressures as high as 8300 kPa. The solids were either silica sand (mean dia $\sim 287\,\mu$m), fluidized by air, or activated carbon (mean dia $\sim 66\,\mu$m), fluidized by a Synthesis gas mixture. Output signals from the gauge were monitored at 100 pt/s with a time constant of 2 ms. In their paper, Weimer *et al.* (1985) discuss the requirements of beam diameter, the balance between detection noise and scan duration and the difficulties in data interpretation. For example, the determination of bubble size is complicated by the unknown path of the beam in relation to the detected bubble (figure 12). Unless the collimated γ-ray beam passes exactly through the centre of the bubble, the vertical diameter of the bubble is underestimated. This can only be rectified by probability analysis. The shape, curvature and shadowing of bubbles create other difficulties in the interpretation. Weimer *et al.* (1985) conclude that γ-ray density gauges allow for accurate measurements of phenomena such as expanded bed height, dense phase voidage, dense phase superficial gas velocity and

centreline bubble phase volume fraction, but that the measurement of bubble size is, at best, approximate.

Seville *et al.* (1986) pioneered the use of a rather primitive γ-ray technique to produce tomographic images (tomograms) of the voidage distribution of the jet region above various gas distributors and under different operating conditions. The system consisted of a single collimated photon beam of 5 mm dia from a 100 mCi Am source and a single NaI detector, aligned on an optical bench with the fluidized bed to be scanned (51 and 146 mm dia), rotated and translated through the beam by a series of stepper motors. 40×2 mm steps were taken at $30 \times 6^\circ$ intervals with 1000 photon/ray-sum collected at each position. This led to total scan times of up to 7.5 h. The complete apparatus was controlled by a microcomputer and the reconstructed images were made up of 5 mm^2 pixels. Calibration between the attenuation and voidage was achieved by scanning a settled bed of material and obtaining a single attenuation coefficient, averaged over the whole cross-section. Without disturbing the bed, the interstitial voids were then slowly filled with water and a second average attenuation coefficient obtained. From the known attenuation coefficient of water, the voidage of the settled bed, and hence the attenuation coefficient of the particles, were obtained.

Initial investigations were centred on the 51 mm dia fluidized bed, 200 mm in height, which could be fitted with two interchangeable distributors; a solid brass plate containing a central 2 mm dia tapered orifice and a porous sintered bronze plate with the same axial orifice but with a separate connection from the orifice for background gas flow through the plate. The static bed height was

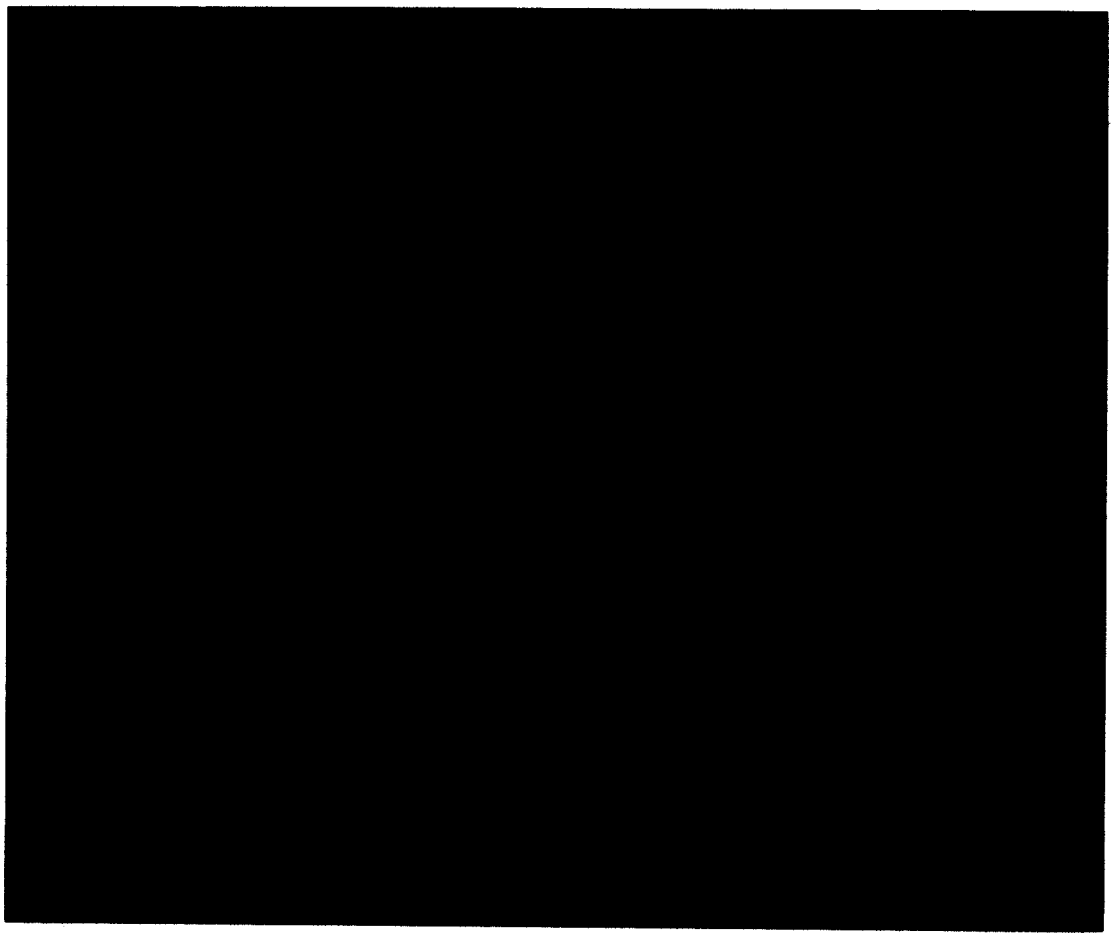

Figure 11. X-Ray image of a single bubble in a group B powder showing regions of varying voidage: black, 0.445; green, 0.495; blue, 0.526; cyan, 0.627; red, 1.0 (Yates *et al.* 1994).

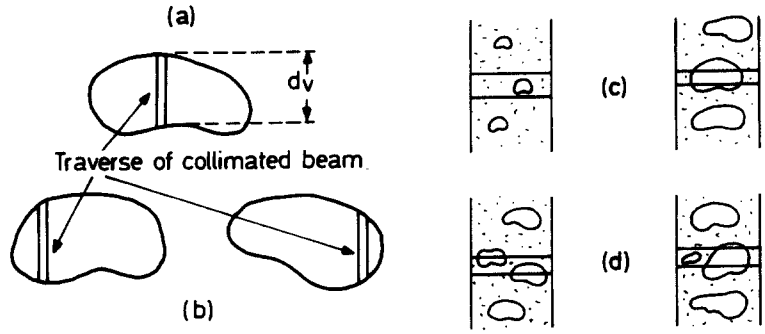

Figure 12. Problems in determining the bubble diameter using a γ-ray attenuation gauge: (a) vertical diameter measured; (b) off-centre intersection; (c) volume effect of intersection; (d) shadowing effect.

60 mm and the bed was scanned at heights 14–40 mm above the distributor. Two bed materials were used; spherical soda glass ballotini (210–250 μm, $U_{mf} = 0.05$ m/s) and angular quartz sand (300–355 μm, $U_{mf} = 0.114$ m/s). The principal objectives of the experiments were to examine the effects of both background fluidization and particle shape on the axial and radial bed voidage profiles. The tomograms and line scans obtained during the investigations clearly indicated the qualitative effects of the two parameters; an increase in background fluidization and a decrease in

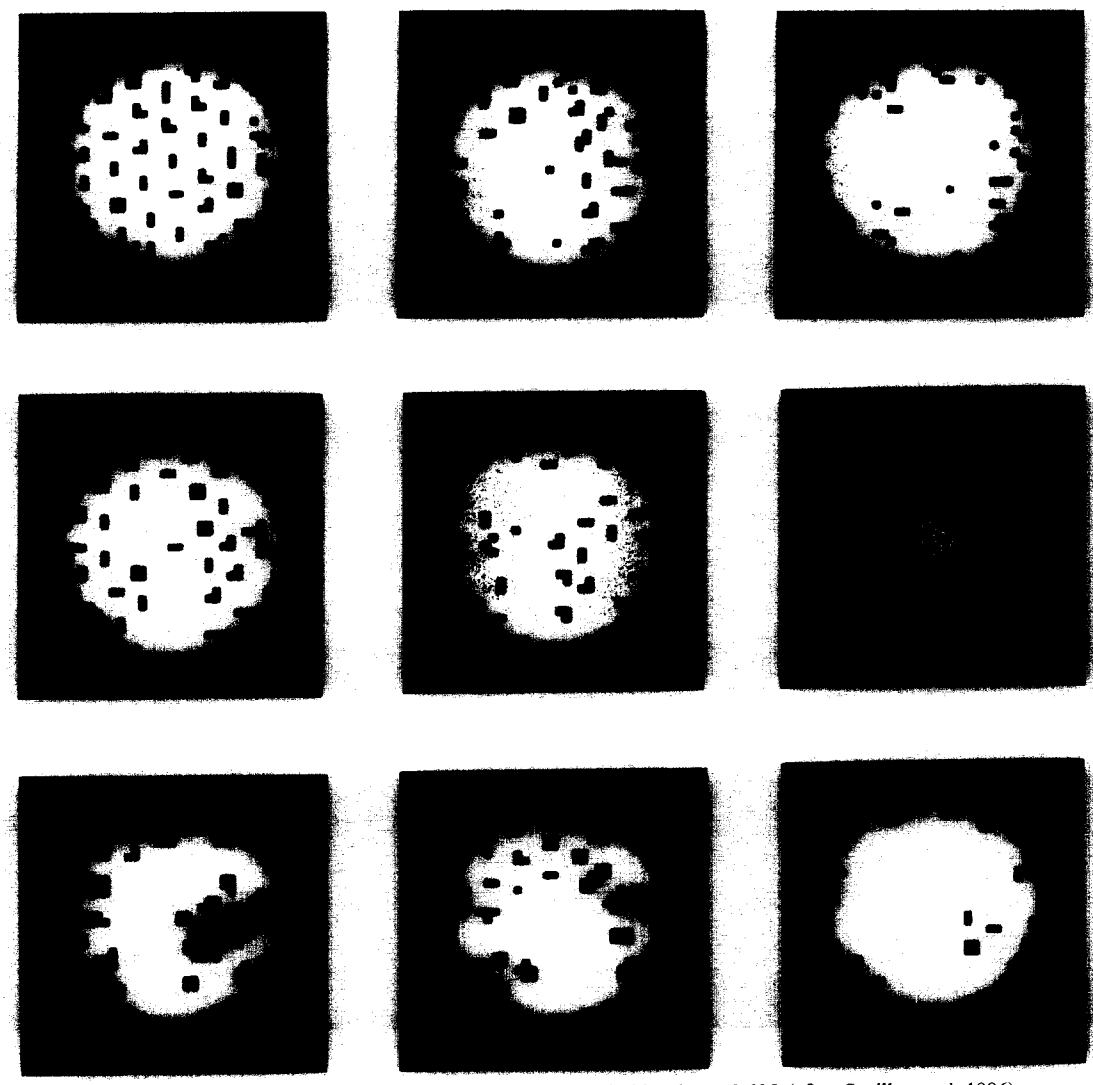

Figure 13. Reconstructed binary bed cross-sections, threshold value = 0.525 (after Seville *et al.* 1986).

particle angularity both cause an increase in the radial extent of the high voidage (jet) region coupled with a decrease in the axial penetration of the jet. These observations are consistent with the conclusion that both background fluidization and high particle sphericity enhance particle mobility and, hence, entrainment into jets, thereby dissipating the jet momentum over shorter distances (Kececioglu *et al.* 1984).

Separate experiments, using the larger 146 mm dia fluidized bed but the same tomographic scanning equipment, were carried out to investigate the effect of increasing gas velocity on jetting and bubbling behaviour. The bed particles were quartz sand (300–355 μm, $U_{mf} = 0.92$ m/s) and the settled bed depth was 150 mm. The distributor was a flat plate with 37 discrete orifices of 1.5 mm dia on a 24 mm triangular pitch, giving a free area of 0.39%. Three different scanning heights were used (20, 30 and 40 mm above the distributor) at three gas velocities (1.38, 2.30 and 3.22 m/s).

To facilitate comparison between the tomographic images, an attenuation threshold value was chosen (0.03/mm corresponding to a voidage fraction of 0.525) below which all pixels were set to black, with the remainder to white. Figure 13 shows the resulting binary images for each of the 9 combinations of experimental conditions. Regions of high average voidage are apparent at 20 and 30 mm above the distributor orifices with $U/U_{mf} = 3.22$ m/s and are also discernible at 20 mm with $U/U_{mf} = 2.30$ m/s. Such images clearly show a decrease in the order of the structure with an increase in the scan height above the distributor (i.e. as the jetting region degenerates into bubble flow) and an increase in the structural detail at all heights as the velocity is increased (i.e. an increase in the jet penetration length with increasing gas velocity). Indeed, Seville *et al.* (1986) compared the jet penetration lengths determined by the γ-ray technique with those predicted using several well-known correlations.

An updated γ-ray tomography device was used by Simons *et al.* (1993) to produce reconstructed images of higher resolution at shorter scan times and with larger diameter vessels than those described by Seville *et al.* (1986). The "scanner" employed an array of 6 ^{153}Gd sources in conjunction with 6 collimated CsI scintillation detectors, all mounted on a fixed gantry with a circular opening through which a 100 mm (maximum) diameter cylindrical column could be lowered and raised. Instead of rotating the object to be scanned through the beam, the scanner ring was moved laterally in steps of 1.0 mm each followed by a rotation of 1.5° around the object until a full 180° was obtained. This resulted in reconstructed images made up of a 155 mm^2 grid of 1.0 × 1.0 mm pixels; for good spatial resolution total scan times were kept around 3–4 h, although scan times in the order of 90 s could be achieved at the cost of resolution. The vessel used in these experiments consisted of a 100 mm dia cylindrical section with a conical base having an inlet orifice of 22 mm dia. The bed material was activated carbon ($U_{mf} = 0.19$ m/s, mean dia = 906 μm), and the bed depth was 550 mm. A superficial gas velocity of $U = 0.37$ m/s ensured that the bed operated in the slugging mode (i.e. with gas bubbles of a diameter comparable to that of the column) and scanning heights of 35, 70 and 200 mm above the orifice were selected to provide images of the cone/jet and bubbling/slugging regimes. For the study of the effects of sticky particle surfaces on the bed structure (Seville 1992), which can lead, for example, to catastrophic defluidization in high-temperature coal gasifiers, a non-volatile viscous oil (200/50 cSt) was added to the bed material.

Only limited information could be obtained by visual inspection of the resulting tomograms. More quantitative analysis was achieved using calibrated line scans of each image. Examples of these are depicted as left-to-right diametric voidage profiles in figure 14(a–d). The differences in the voidage profiles in each plane and between the dry and sticky beds are clearly defined. However, a major disadvantage of using this type of scanner is the time-averaged nature of the measurements, which limits the usefulness of this technique in process diagnostic applications.

2.2.3. Capacitance imaging

The principle of capacitance measurement in gas–solid and solid–liquid systems was described earlier in relation to the use of capacitance probes in fluidized bed investigations. However, several workers have avoided the problem of probe interference by using externally mounted capacitance plates, notable contributions being those of Ormiston *et al.* (1965), who used two sets of capacitor plates to measure slug velocities, and Halow & Nicoletti (1992), who used capacitance tomography to image bubble behaviour.

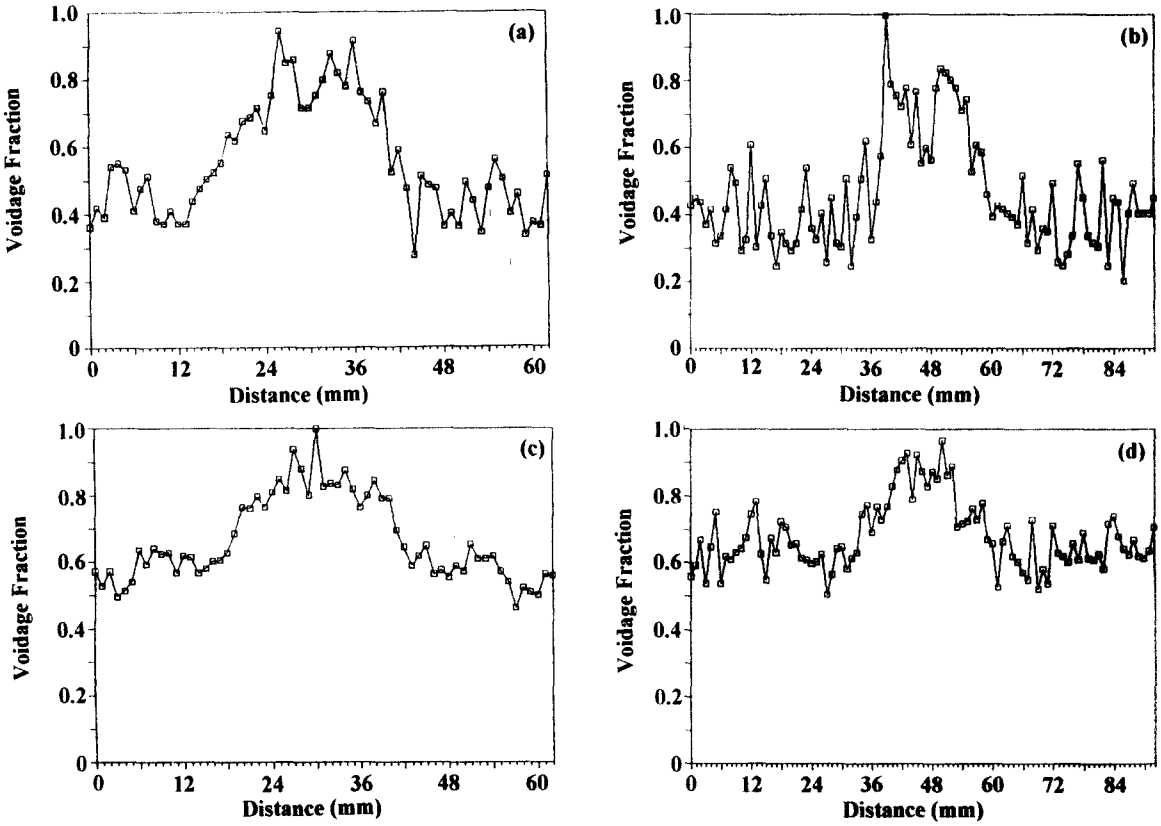

Figure 14. Diametric voidage profiles of a jet in a fluidized bed (coinical base, 100 mm dia, cylindrical section) at: (a) 35 mm (b) 70 mm from orifice, dry solids; (c) 35 mm (d) 70 mm from orifice, sticky solid.

Ormiston *et al.* (1965) attached two sets of capacitor plates to the outside of perspex columns of various diameters (25–140 mm), the two sets spaced approximately 25 mm apart in the vertical direction. The bed heights were 100 mm in the smaller diameter columns and 500 mm in the largest diameter column and the detecting plates were fixed close to the upper surface of the bed. Two types of sand (mean dia = 108 and 254 μm, respectively) and catalyst particles (mean dia = 41.5 μm) were used as the bed materials. The change in the capacitance of the plates due to the passage of a slug was detected by proximity meters, one for each set of plates. A counter in a bi-stable circuit was activated as the slug passed the bottom set of plates, then stopped as the slug reached the upper set, the circuit effectively acting as an automatic stop-watch. Precautions were taken against stray capacitance (copper shields around the plates), current leakage along the perspex columns (earthed screens) and the electrical conductance of the bed (modified by adding resistor–capacitor networks), which would lead to charge loss [see, for instance, Simons & Williams (1992)]. The objective was to compare the slug velocities in gas-fluidized beds with those predicted by theory for gas slugs in water-filled tubes. The results showed close agreement and were confirmed by X-ray analysis (the UCL facility), which also showed that slugs were of the same shape in both types of system.

Since the 1970s, Halow and co-workers at the Morgantown Energy Technology Centre (WV, U.S.A.) have been conducting extensive research on the use of capacitance techniques to measure bed levels, solid flow rates and gas bubble phenomena in fluidized beds. These efforts have evolved into a highly sophisticated capacitance tomography system, recently reported in detail (Halow & Nicoletti 1992), which is capable of imaging in three dimensions the voidage distribution within fluidized beds at rates of 60–100 frames/s. The imaging system comprises 4 sets of 32 electrodes fixed at various positions along the vertical height of a 152 mm dia column. The resultant images allow the direct observation of bubble coalescence phenomena and the interpretation of data such as bubble rise velocities, bubble size and voidage distributions in the emulsion phase. Figure 15 is an example of a 3-D image showing bubble coalescence, in which the lower bubble appears to

drain into the upper bubble. These images are constructed by having a cut-off value of void fraction, below which is defined as emulsion phase and above which is defined as bubble phase. A cut-off point between 0.70 and 0.75 has been selected in this case, with the colours white and yellow corresponding to high void fractions and blues and magenta to void fractions near that at minimum fluidization. Thus, in the first frame of figure 15 a large slug is visible in the upper imaging levels. In successive frames, a following void extends a central spike to the lead slug and then elongates and rises along this spike to coalesce with it. Other, similar tomograms have revealed how the average voidage between bubbles is higher than that at minimum fluidization and is dependent on the superficial velocity and that the voidage of the emulsion phase is not uniform anyway, but consists of channels of higher or sometimes lower voidage than the surrounding interstices. These observations have obvious ramifications on existing modelling procedures and current theories of the solids–gas flow behaviour. The two-phase theory, for instance, is clearly inadequate to describe the complex phenomena visualized by the capacitance tomographic technique. The main limitations of the technique, however, are the poor resolution (of the order of 10 mm in the cross-sectional plane and 25.4 mm in the vertical dimension), the blurring of voidage boundaries (due to the effect of averaging the measured electrical permittivities) and the uncertainties, prevalent in all tomographic techniques, relating to the deconvolution of the current measurements. Effects such as "ghosting" or false images can occur, especially when there are more than two objects within the same imaging field. Thus, when two bubbles are present in this manner, a false increase in the voidage of the region between them will be indicated. Nevertheless, the applicability of electrical sensing imaging to fluidized systems has been demonstrated and the continued evolution of powerful computers and of instrumentation technology will eventually lead to the relaxation of the limitations.

3. METHODS FOR STUDYING PARTICLE DYNAMICS

Particles circulate and mix in fluidized beds under the influence of gas bubbles. Bubbles carry particles behind them in their wake and these are deposited on the bed surface or thrown into the freeboard region when the bubbles erupt; particles in the bed region outside the bubbles thus tend to move downwards to compensate for this net upward drift and this sets up circulation patterns that are a reflection of the bubble flow. The high degree of solids mixing this produces is responsible for the excellent heat transfer properties of fluidized beds and is one of their more attractive features as a processing tool. As the fluidizing gas velocity increases, bubbles grow to such a size that they either form slugs that fill the bed cross-section or become unstable and break up into smaller entities; whichever of these occurs depends on the physical properties of the particles and the dimensions of the bed.

3.1. Use of Tracer Particles

3.1.1. Colour and size difference

Before the advent of the sophisticated radiation systems that are available today, the mechanisms of solids mixing in fluidized beds were investigated using laborious techniques which involved either following the random motion of one or two selected particles (marked in some way, i.e. by colour and/or size) with ciné photography, or sectioning the bed from time to time during the mixing of two differently coloured (and/or sized) batches of solids. Rowe *et al.* (1965) give a brief review of the former technique and a more detailed description of the latter, which will now be discussed here.

Tracer material can be arranged easily as a layer in the bed at the start of an experiment or, in a continuous system, the feed composition can be altered at a chosen time interval. After fluidizing the bed for a certain time, the gas can be turned off and the bed dissected at leisure to examine the tracer movement. It is the dissection of the bed which is the most tedious part of the technique. The simplest method is to remove the particles, by vacuum, as shallow layers from the bed, and then analyse the sample for tracer material. Kececioglu *et al.* (1984) used this method in their study of the fate of solids fed pneumatically into a fluidized bed. In this case the tracer particles were of a much coarser mean size than the bed particles (2850 μm as opposed to 770 μm), but of the same density, and therefore it was assumed that no segregation would occur. The tracer

particles were added to the main gas stream via a screw feeder and injected into the bed over different time intervals, after which the bed was instantly defluidized. The bed was then sampled layer by layer to obtain the radial and axial concentration profiles of the tracer. The tracer particles were recovered from the main bulk material by sieving and the concentration of each layer recorded. Kececioglu *et al.* (1984) presented their data in terms of the ratio of concentration of tracer in the sample to the total concentration of tracer in the bed vs axial location. In this way a degree of mixing could be ascertained, a uniformly mixed bed having a ratio equal to unity. Furthermore, to give an indication of deviation from the uniformly mixed state, a root-mean-square concentration deviation was defined as

$$d_{\text{r.m.s.}} = \left[\frac{1}{V} \int_0^V (C_T - 1)^2 \, dV \right]^{1/2}, \qquad [15]$$

where V is the volume of sampled bed solids and C_T is the concentration ratio defined above. The results indicated that the higher the jet velocity and the longer the fluidizing time period, the better the mixing and that in the region around the jet in the conical distributor, solids mixing was not adequate. This supported visual observations made by the same authors of a "zone of influence" of the jet centred around the inlet orifice.

The technique of sectioning the bed layer by layer to reveal mixing patterns has been used extensively by Nienow and co-workers. Their studies were focused on the effect of particle segregation on mixing patterns in systems containing bi- and tri-modal and polydisperse size distributions. The work is reviewed in detail by Nienow & Chiba (1985), who categorize segregation phenomena by the tendency of the components either to rise (the flotsam) or to sink (the jetsam), thereby leading to a variation in concentration from the top to the bottom of the bed by either size or density. For flotsam-rich systems, the tracer technique revealed a layer of pure jetsam at the bottom of the bed at velocities just above U_{mf}, whilst the upper part of the bed contained a fairly uniform distribution of jetsam in low concentrations. Such behaviour was not repeated in the converse situation of jetsam-rich systems, there being a gradual change in composition with bed height with no flotsam-rich layer at the bottom of the bed. Increasing the gas velocity improved mixing.

Rowe *et al.* (1965) described a more complicated, vertical sectioning technique in their study of solids mixing in more conventional fluidized beds. They used mixtures of monodispersed size, iron-coated, lead glass and soda glass ballotini (mean dia = 460 μm) in a 0.13 mm dia perspex bed. The lead glass could be identified either visually by its dark iron-coating or by X-ray images as the more radiographically denser particles. Experiments were carried out with the bottom half of the bed initially consisting solely of lead glass and the top half solely of soda glass. Single gas bubbles were then injected into the bed, by maintaining the bed at the minimum fluidization velocity and then injecting a pulse of air through a separate orifice in the distributor to form a bubble of chosen size at the required time. X-ray ciné photography was then used to obtain sequence images of the effect of the single bubble as it rose through the bed, the wake and drift volumes being made up of lead glass ballotini. More bubbles could then be injected so that the change in mixing patterns could be followed.

After each experiment the bed was sectioned vertically to show the pattern left behind by the bubble(s). The procedure was as follows. The perspex vessel was made of two semi-cylindrical shells bolted together. One of the shells had a vertical slot 0.7 cm wide, extending within 3 cm of each end and 90° to the diameter dividing the two halves. This slot was sealed (with Sellotape) during fluidization. Once fluidization had ceased, the bed was clamped into position with a metal disc and then turned onto its side with the slot uppermost. The Sellotape was then cut away and the particles in the upper semi-cylindrical section removed by a hand-held suction tube. The upper section was then parted from the lower one and a level plane was finally obtained by setting the suction tube at a fixed height and working patiently over the particulate surface. The section was also photographed for permanent record. This technique required great care and patience, but the revealed patterns clearly showed the effect of bubble motion, wake and drift on the solids mixing. Indeed, the information gathered by such investigations has been used to produce the models of solids circulation rate and bubble wake and drift volumes so familiar today.

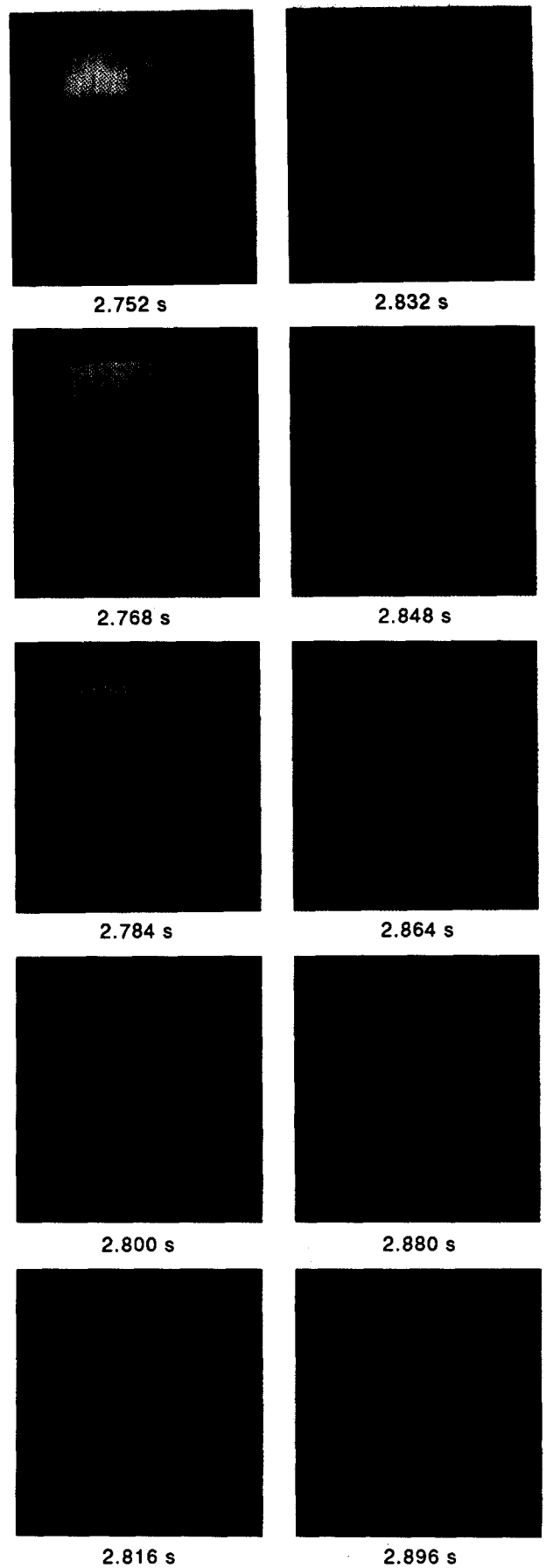

Figure 15. 3-D capacitance tomography images illustrating bubble coalescence (Halow, private communication).

3.1.2. Positron emission tomography (PET)

PET is well-established as a medical imaging technique but has only recently been applied to laboratory-scale process diagnostics by researchers at Birmingham University. Installed in 1984 for the purpose of studying lubrication in engines and gearboxes, the Birmingham positron camera remains the only PET facility dedicated to non-medical imaging and, with positron-emitting radionuclides produced "in-house" using the two cyclotrons belonging to the university, has been used for a wide range of (process) engineering studies, including particle motion in fluidized beds (Simons *et al.* 1993).

The principles of the technique and the design of the camera itself are described fully elsewhere (Parker *et al.* 1993); in brief, the coincident detection and location of γ-rays resulting from the annihilation of a positron (emitted by the tracer) by an electron within the field of view of the

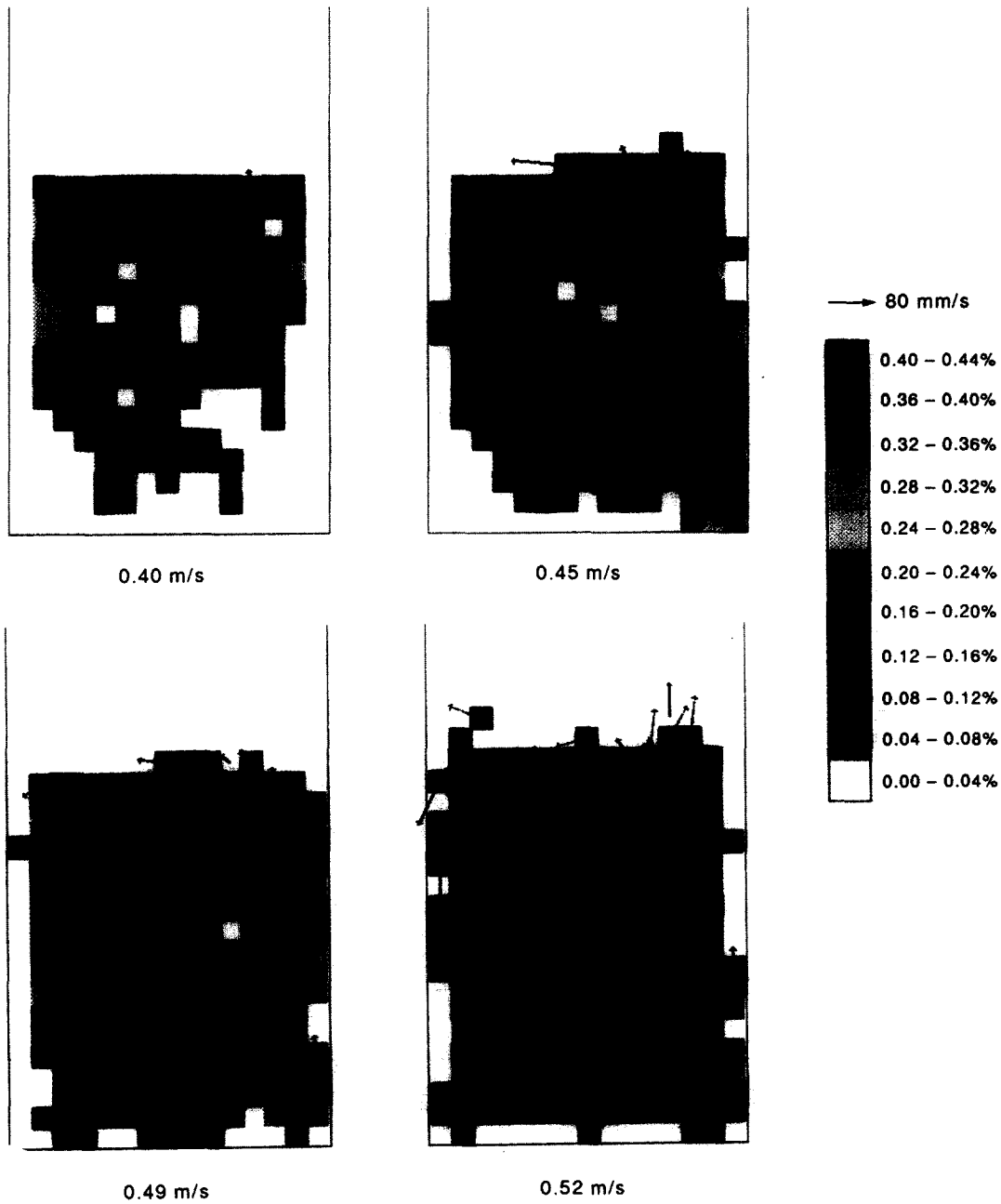

Figure 17. Spatial distribution and velocity field in the transaxial plane of a fluidized bed at different superficial gas velocities obtained by positron emission particle tracking.

positron camera enables the reconstruction of the path taken by the two γ-rays, which in turn leads to the construction of an image. From a number of such detections and reconstructions, the location of the positron emitter can be estimated (figure 16). The positron camera itself consists of two position-sensitive detectors, each with an active area of $600 \times 300\ mm^2$, mounted on either side of the field of view. Each detector consists of a multiwire proportional chamber with an efficiency of approximately 7% in detecting an incident 511 keV γ-ray. The separation of the detectors can be altered to suit the size of the object being studied.

Only coincident events in which γ-rays are registered in both detectors are accepted and stored on disk, together with the co-ordinates of both γ-rays and the time of detection. In practice, due to Compton scattering, not all the reconstructed γ-ray paths cross at a single point. A particle tracking algorithm, developed by Parker *et al.* (1993) specifically to track a particle moving in an erratic fashion, discriminates against these corrupt paths. The algorithm also selects a suitable interval of data as the initial set of coincidence events. Too short an interval results in poor location resolution due to inadequate statistics, whereas too long an interval will give results distorted by the movement of the tracer. The precision of location also decreases with increasing tracer velocity. Thus, in the fluidization studies (Simons *et al.* 1993), where approximately 2000 event/s were detected, of which 90–500 were required to locate the particle, the uncertainty of location in three dimensions varied from 3 to 7 mm up to a velocity of 1 m/s. This uncertainty is always dominated by the uncertainty in the co-ordinate normal to the detector faces (figure 16), so the precision in the other co-ordinates will be considerably better.

Positron emission particle tracking can provide real-time data on local particle motion which will prove invaluable in the development of mathematical models for design purposes. Figure 17 is an example of the radial and angular distributions of a single 2 mm dia ^{18}F silica tracer (with an initial half-life activity of 300 μCi) within a 150 mm dia fluidized bed of coarse granular sand (average particle dia = 1 mm, bed depth = 150 mm) (Simons *et al.* 1993). The bed was fluidized over a range of superficial gas velocities (U_s), from 0.40 to 0.52 m/s, via a flat-plate distributor. The spatial distribution of the tracer is presented as a 10-point colour scale representing the fraction of time the tracer spent in each of an array of 10 mm^2 bins. The length of the velocity arrows is proportional to the average velocity of the tracer, again in each of an array of 10 mm^2 bins. The increased agitation and improved mixing of the bed with increasing velocity can clearly be seen. From the wealth of information obtained from PET in tracking single particle motion, quantitative information on other phenomena, such as particle collision velocities and residence times, can also be determined.

3.1.3. Other radiation techniques

There are other radiation techniques which have been used by researchers studying solids behaviour in fluidized beds. Most of these involve crude forms of tracing radioactive particles [Table 13.5 in Geldart (1986) provides a comprehensive listing]. For example, Littman (1964) dosed a 50 mm dia bed of copper spheres with an irradiated 10 g charge of ^{64}Cu spheres and measured the activity in the bed during fluidization, using an NaI scintillation counter, until a steady state had been reached. Two indices of the rate of solids mixing were then defined; namely,

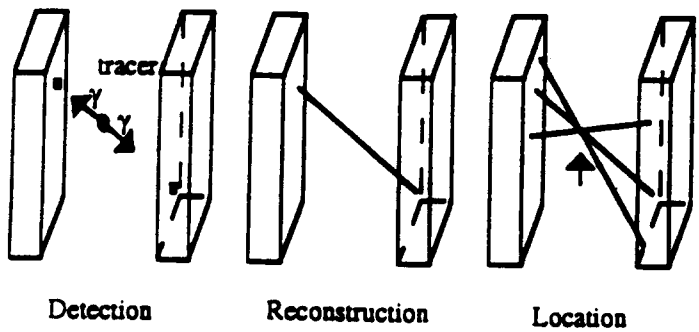

Figure 16. The detection and reconstruction of coincident γ-rays leading to the location of the tracer particle in the Birmingham positron emission camera (after Broadbent *et al.* 1993).

the time required to uniformly disperse the activity charged to the bed and the velocity of the activity front.

In another study, Merry & Davidson (1973) used a 20 mm dia "radiopill", consisting of a transistorized oscillator in a hollow perspex shell, to measure particle velocities at the centre of a 250 mm deep bed fluidized by an uneven air flow to form the so-called "Gulf-Stream" circulation pattern. However, there were two major disadvantages with the method used: (i) the behaviour of the very large tracer could not be compared to that of the bed particles (mean particle sizes ranging from 50 to 300 μm) with any real degree of certainty; and (ii) the presence of the radio receiver, which took the form of an aerial network mounted in the bed, severely disrupted the bed hydrodynamics.

A complex, though ingenious, imaging technique for following the motion of a radioactive tracer in a fluidized bed was developed by Lin *et al.* (1985). Their apparatus consisted of 12 photomultiplier detectors mounted in a staggered configuration at 3 different heights around a perspex column of 138 mm dia. As the tracer particle, made of ^{46}Sc with a diameter similar to that of the glass beads used as the bed particles, moved around the bed, its γ-radiation was continuously monitored by the detectors, the count rate at each detector being interpreted by a computer to yield the distance between the tracer and that detector. Instantaneous location of the tracer was then determined by triangulation of the 12 distances.

For the purpose of determining mean velocity distributions, the bed was divided into 154 sampling compartments and, by running the experiments for sufficiently long durations, the repeated appearance of the tracer in a given compartment enabled ensemble averages of the instantaneous velocities to be calculated. For a typical running time of 2 h using a sampling interval of 30 ms a total of 240,000 data points were obtained. Mean velocity distributions were then summarized in vector diagrams similar to those obtained using the PET technique described above (i.e. figure 17).

3.2. Solids Flow in High Velocity Risers

At velocities approaching the terminal velocity of the particles, fluidized beds pass into the so-called turbulent regime where well-defined bubbles no longer exist and where much of the solid material is carried out of the bed altogether. In order to maintain a constant solids loading in the bed it is then necessary to collect the particles in an externally mounted cyclone and to recycle them via a standpipe and some throttling device, such as an L-valve, back into the base of the original bed. Systems such as this are called circulating fluidized beds, or CFBs, and the type of fluidization occurring in the bed (or riser) is referred to as "turbulent" or "fast". Two very important industrial applications of this type of operation are in the FCC process and in CFB combustion. Industrial CFB units are very large; a typical cylindrical FCC riser would have an internal diameter of 1 m and a height in excess of 20 m, while a CFB combustor would have a square cross-section with a hydraulic diameter of 5 m and a height of 30 m (Werther 1993).

The movement of solid particles and the attendent gas flow patterns in these high-velocity beds are of particular interest and they have been the subject of a large number of experimental studies in recent years. Most detailed studies have been carried out on laboratory-scale units, although there is considerable doubt as to whether the solids flow patterns observed in them are in any way similar to those occurring in industrial CFB reactors (Werther 1993).

3.2.1. Solids concentration profiles

The early work on turbulent and fast fluidization was reviewed by Yerushalmi & Avidan (1985) and by Geldart & Rhodes (1986). These studies were mainly concerned with establishing the existence of this type of fluid bed structure and with exploring the differences between it and the more familiar bubbling regime. Measurement techniques used in these early studies included capacitance (Lanneau 1960; Kehoe & Davidson 1971; Massimilla 1973; Canada *et al.* 1976) and pressure variation [the City College, (New York, U.S.A.) work reviewed in Yerushalmi & Avidan (1985)]. Subsequent work has been directed at quantifying the axial and radial solids distributions in turbulent beds and a number of different techniques have been employed.

The use of fibre-optic probes was pioneered by Okhi, Shirai and co-workers in the mid-1970s (Okhi *et al.* 1975; Okhi & Shirai 1975) and was subsequently developed to measure particle

concentrations in fast beds by Qin & Liu (1982). The latter workers used a probe with a $2 \times 2\,mm^2$ surface consisting of alternating layers of optical fibres, one layer providing a source of light and the other receiving the light reflected back from the bed particles; the illuminating fibres were connected to a laser and the receiving fibres to a photomultiplier and associated electronics for data analysis. A similar probe consisting of 700 fibres was described by Hartge *et al.* (1986); again half the fibres were light-emitting and half light-receiving. The output voltage from the probe was found to be linear in solids concentration, a fact that was checked by connecting it to a liquid fluidized bed in which the radial solids concentration was varied by varying the liquid flow rate through the bed. In view of this linearity of response, the probe was calibrated by fixing two points on a scale of solids concentration in a fast bed riser: the first point was obtained from the empty tube and the second by traversing the probe over the diameter of the fast bed under operating conditions; the average voltage from the probe, $\bar{U}$, was then compared with the average solids holdup, c, calculated from the differential pressure drop at that bed level. The calibration line was then determined from the two points $\bar{U}(c)$ and $U_0(c = 0)$. Figure 18 shows results obtained by Hartge *et al.* (1986) using the probe to measure axial solids distributions in a 0.4 m dia CFB at two gas flow rates, 4.0 and 4.2 m/s, and two solids fluxes, 64 and 90 kg/m^2s. The existence of a lower relatively high-density region and an upper low-density region are clearly apparent, as is the good fit of the results to the model equation proposed by Kwauk and his co-workers (Li & Kwauk 1980).

$$\ln\left(\frac{\varepsilon - \varepsilon_a}{\varepsilon^* - \varepsilon}\right) = -\frac{1}{z_0}(z - z_i), \qquad [16]$$

where ε is the average voidage across a diameter, ε^* and ε_a are the limiting voidages in the dilute and dense regions, respectively, and z_0 is a fitting parameter, the so-called "characteristic length" of fast fluidization.

Radial solids concentration profiles were measured by Qin & Liu (1982) and by Hartge *et al.* (1986), although a more comprehensive study was carried out by Zhang *et al.* (1991) using the same optical probe as was used by Qin & Liu (1982). The main difference between the work of Zhang *et al.* and that of the previous workers was in the method used to calibrate the probe which, in their opinion, did not respond linearly to the solids concentration in a gas-fluidized bed. The method was as follows. Approximate values of the cross-section-averaged voidage $\bar{\varepsilon}$ were found from differential pressure drop measurements in the normal way, although readings were made with a frequency of 25 Hz simultaneously with probe measurements along the bed radius. Readings from the probe at each of 9 points along the radius of their 90 mm dia riser were integrated over a 1 min period and the average intensities at each point were determined. The non-linearity of the bed voidage was then expressed as

$$\varepsilon = C_0 + C_1 S + C_2 S^2 + \ldots + C_k S^k, \qquad [17]$$

where S is the signal intensity at a point. The local time-averaged voidage, $\varepsilon(\phi)$, at points along a radius can then be calculated from [17], given the values of the coefficients. The average voidage for a particular cross-section will be

$$\bar{\varepsilon} = \int_0^1 2\phi\varepsilon(\phi)\,d\phi. \qquad [18]$$

For a number of runs under different conditions, say 10 in all, the readings of $\bar{\varepsilon}$ from the pressure drop measurements and the corresponding optical signal profiles will form a system of 10 simultaneous equations that may be solved to give the coefficients C_0, C_1 etc. Figure 19 shows the values obtained for three fluidization regimes using the method; the generally accepted radial structure of the fast fluidization regime with a lean core and a dense annulus is clearly apparent.

Horio *et al.* (1992) used an optical fibre probe to study the transition from turbulent to fast fluidization in a 50 mm dia riser. The probe was calibrated to measure local voidages and also to determine the size of particle clusters, which are thought by some investigators [but not by all—see Geldart & Rhodes (1986)] to be formed under high-velocity conditions. Axial voidage profiles similar to those reported by Hartge *et al.* (1986) were found and it was shown that the voidage

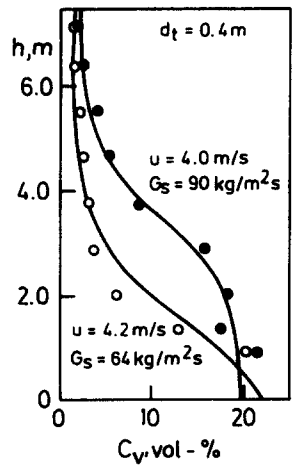

Figure 18. Vertical density profiles in a fast fluidized bed riser (Hartge *et al.* 1986).

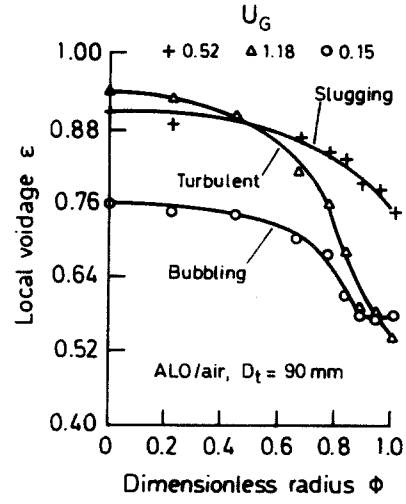

Figure 19. Radial voidage distributions for three regimes in a fast fluidized bed riser at two gas velocities (U) and two solids fluxes (G_s) (Zhang *et al.* 1991).

gradient at the inflection point $(\delta\bar{\varepsilon}/\delta z)_{inf}$ decreased with increasing gas velocity and then became constant at some velocity which marked the transition from turbulent to fast fluidization (figure 20). It was also shown that the cluster size decreases with increasing gas velocity in both regimes.

The application of γ-rays to high-velocity fluidized systems has been developed extensively by the oil companies, notably Shell and Esso, to provide quantitative measurement of the solids concentration and distribution, particularly in catalytic crackers (Bartholomew & Casagrande 1957; Saxton & Worley 1970), and this work is still being perfected today by researchers at Elf (Martin *et al.* 1992).

Bartholomew & Casagrande (1957) have reported on the use of γ-ray attenuation to determine density (or concentration) patterns of fluidized systems in transfer lines and vessels ranging from 0.15 to 12 m dia and have described how catalyst density contours were obtained from certain elevations on a 0.5 m dia vertical catalyst riser. The radioactive source, uncollimated ^{60}Co (5 mCi), and the detector, an uncollimated Victoreen 1B85 Geiger–Müller tube (for practical simplicity) with preamplifier and scaler, were positioned at 18 consecutive points around the riser, execution of the path measurements requiring approximately 1 h. The data were converted directly to mean path densities using equations derived from the Lambert–Beer law of exponential absorption. Small

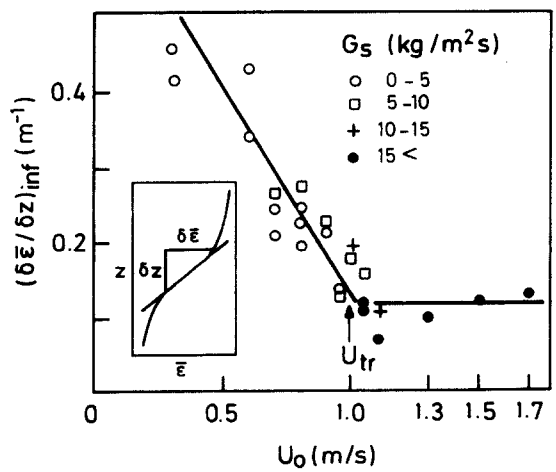

Figure 20. Voidage gradient at the inflection height in a fast fluidized bed of cracking catalyst at four solids fluxes (G_s) (Horio *et al.* 1992).

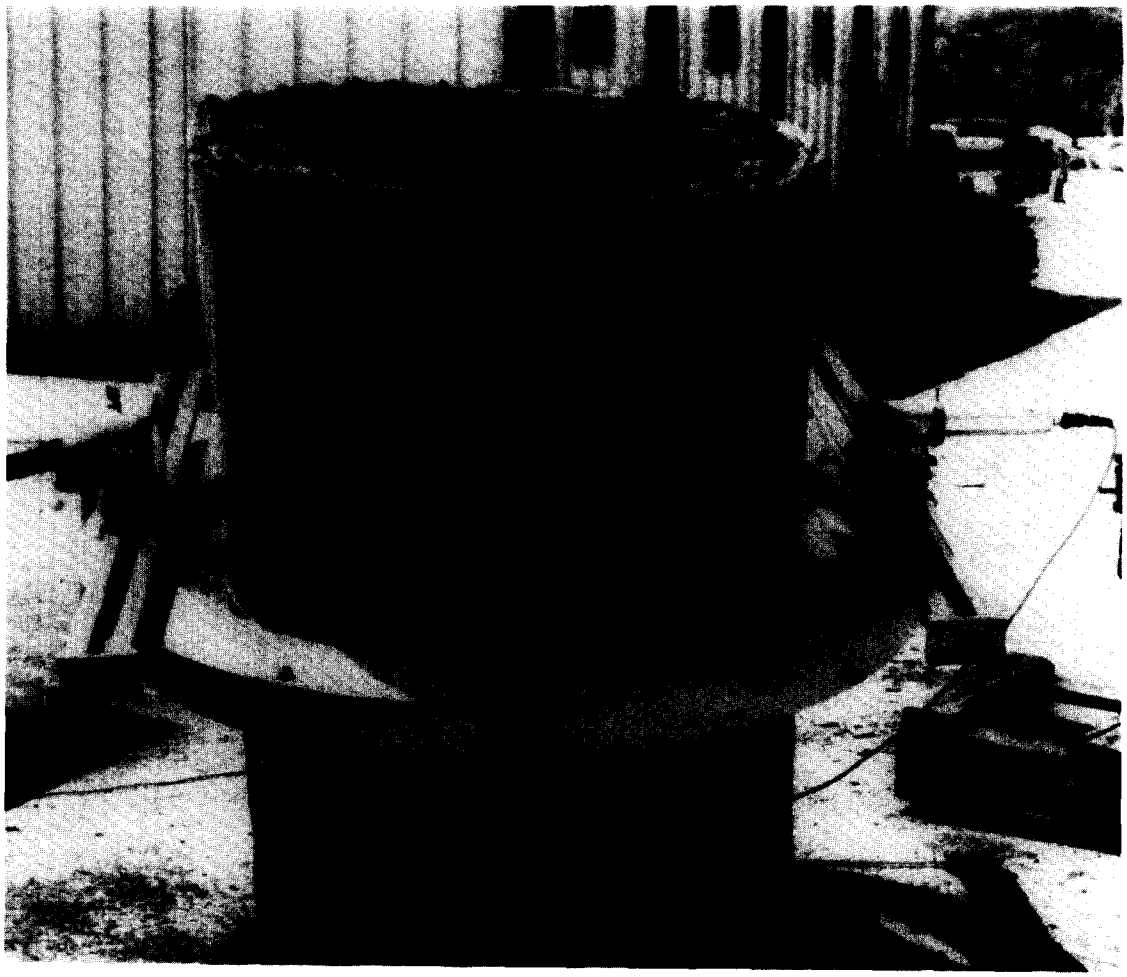

Figure 21. γ-Ray tomography apparatus on a section of riser (courtesy of Elf).

corrections for coincidence losses and background noise were made on all counting-rate data. Actual construction of the density contours was achieved analytically by a Cartesian co-ordinate system.

Similar density contours have been reported by Saxton & Worley (1970). In both cases, low-velocity–high-density regions were indicated near the vessel walls, whereas the converse was true near the centreline. The degree of contacting, indicated by the catalyst distribution, improved as the catalyst–gas mixture travelled up the riser, whilst tests on oil–feed nozzle configurations revealed improvement when the number of nozzles was increased from 1 to 3. Such data has been used in the evaluation of the effect of equipment-design variables on catalyst behaviour and on process results in the reactor, stripper and regenerator and to set design criteria and operating guidelines.

More recent work on FCC risers has been reported by Turlier and co-workers, who have developed a γ-ray device to obtain tomographic images and 3-D density maps of riser cross-sections. The preferred radiation source is ^{137}Cs (500 mCi), with the detector being a lead-collimated (30 mm dia opening) NaI scintillator. The scanning apparatus, shown in figure 21, can be used on objects up to 1.2 m dia and allows for any number of rotations and translations. For instance, figure 22 is a catalyst density map of an industrial riser, taken with 3 rotations $\times$ 9 translations., In this case the solids mass flux is 1090 kg/m^2 s and the superficial gas velocity if 25 m/s. The mean surface concentration near the wall is 270 kg/m^3, whilst the mean core concentration is 50 kg/m^3, i.e. the profile follows that of the well-known core-annulus structure of circulating beds (Martin *et al.* 1992). For higher resolution tomograms more rotations and translations are required. Generally, 18 rotations and 11 translations have been used, complete scans taking up to 2 h (Desbat

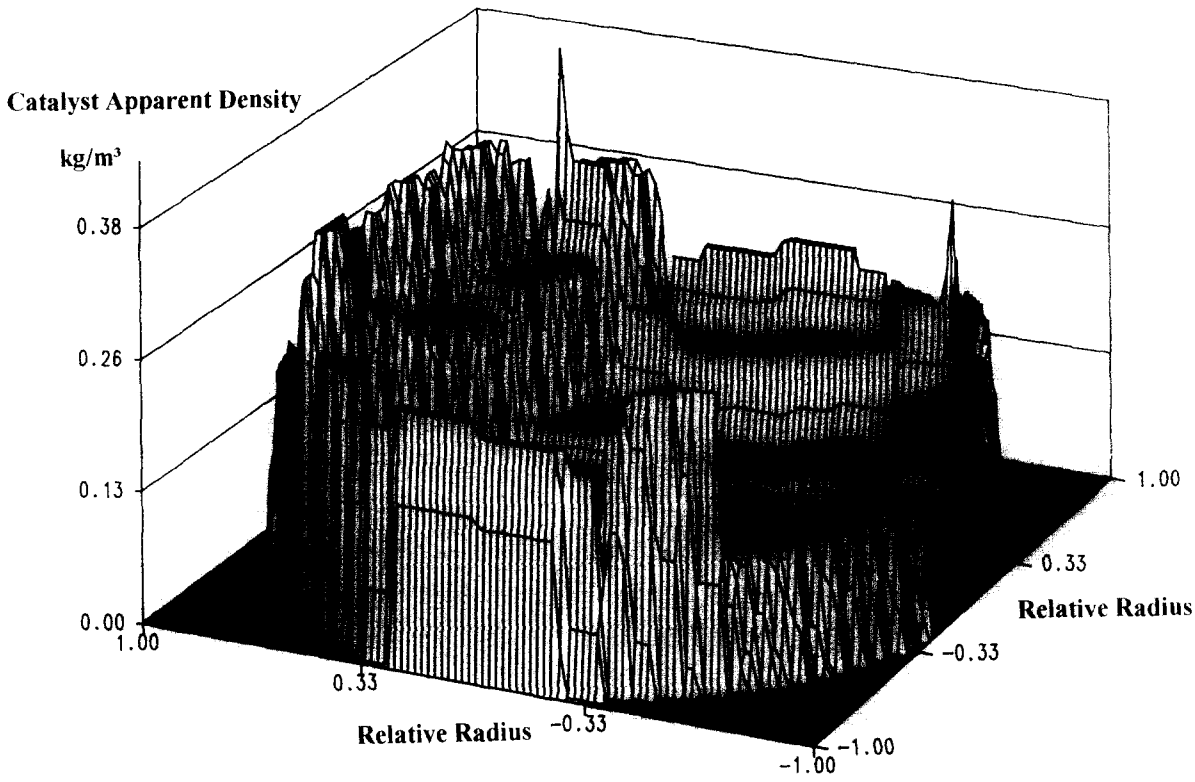

Figure 22. Catalyst density map in a 1.2 m dia riser determined by γ-ray tomography (Martin *et al.* 1992).

& Turlier 1993). However, in practice, 1–2 days are required to avoid any errors in interpretation. Other practical problems include the amount of space required for the equipment (e.g. for a riser of 1.1 m o.d., a free area of 2.3 m dia is necessary) and the radiation hazard from the high-intensity source. Such an intensity is useful for obtaining good precision in counting rates, but operation of the device therefore necessitates a delimited safety area and/or operation at night.

Weinstein *et al.* (1992), at City College (New York, U.S.A.), are currently employing X-ray attenuation techniques in the study of solid–gas behaviour in fast fluidized bed systems. Their X-ray apparatus consists of a Norelco MG 150/300 X-ray generator operated with a 150 keV tubehead mounted on a carriage which can be raised or lowered over a 4 m riser section (150 mm dia) of the college's fast fluidized bed facility. Plate or movie film exposures can be taken to give "instantaneous" snapshots of the radial solid fraction distributions at a selected axial position. The data is then converted to cross-sectional average values of solid fraction using a chordal absorptometry technique. Results have shown that dilute core and dense wall regions are a characteristic of fast fluidized bed systems.

3.2.2. Solids mass fluxes in circulating beds

The overall flux of solids circulating in a high-velocity system can be measured by collecting the total flow over a fixed period of time and weighing. Alternatively, the flow may be sampled on-line by incorporating a load cell into the equipment, as described by Horio *et al.* (1992). The solids flux in the riser itself is rather more difficult to determine, since the solids flow is vertically upwards in the core region and overall downwards in the annulus close to the wall; also, solids exchange occurs between the two regions. It is thus necessary to remove solids from different positions within the riser using some kind of sampling probe; to date, relatively few studies of this sort have been attempted.

Isokinetic sampling, in which suction is applied to a probe at a flow rate equal to that of the local gas stream, is widely used to measure solids fluxes in flowing dusty gases. However, as has been pointed out by Rhodes & Laussmann (1992), such a technique may not be appropriate for

turbulent and fast risers, where the local gas flow rate can be zero or where the solids flow is against the gas flow. Rhodes *et al.* (1988) had previously demonstrated that the net solids flux, i.e. the difference between fluxes measured upstream and downstream at a point, was independent of the suction velocity of the probe tip, provided the gas velocity in the sample lines was sufficient to prevent blockages. Figure 23 is a schematic of the sampling system used by Rhodes & Laussmann (1992) and shows the semi-circular-shaped probe and its associated vacuum lines. The probes were made from stainless steel tubing of 6.3 mm o.d. and 4.9 mm i.d. The net solids flux was found by subtracting the upward and downward fluxes with the probe positioned appropriately and with the same suction velocity.

A probe designed to sample flowing solids isokinetically was described by Herb *et al.* (1992). This consisted of a 5 mm i.d. stainless steel tube curved through a right-angled elbow and fitted with small pressure tappings inside and outside the probe tip; under isokinetic sampling conditions, the difference in pressure between the inside and outside should be zero. The probe was connected to a vacuum collecting system, somewhat similar to that described by Rhodes & Laussmann (1992), and was used to measure solids mass fluxes in laboratory- and pilot-scale units. Herb *et al.* (1992) found clear evidence of a core-annular structure in both risers, the central core region being dominated by a dilute upflowing suspension of solids flowing at high velocities. Although the annulus was occupied by a dense relatively low velocity downflowing solids suspension, an upward solids flux was detected in this region which intermittently interrupted the overall downward flow.

By combining their density measurements obtained via γ-ray attenuation (see above) with those from a momentum probe, Martin *et al.* (1992) were able to estimate catalyst velocity and flux profiles in FCC risers, the results showing high flux values at the centreline and low values towards the walls.

3.2.3. Particle velocities

Several reports have been published of measurements of particle velocity in circulating risers. A common technique is to use optical probes containing light-emitting and light-receiving fibres which detect the movement of particles in their vicinity by light reflection. Cross-correlation of the signals from two probes then enables particle velocities to be measured directly (Horio *et al.* 1988, 1992; Militzer *et al.* 1992).

Laser-Doppler anemometry has also been used to measure particle velocities (Levy & Lockwood 1983; Arastoopour & Yang 1992). The basis of the technique is that the frequency of light scattered

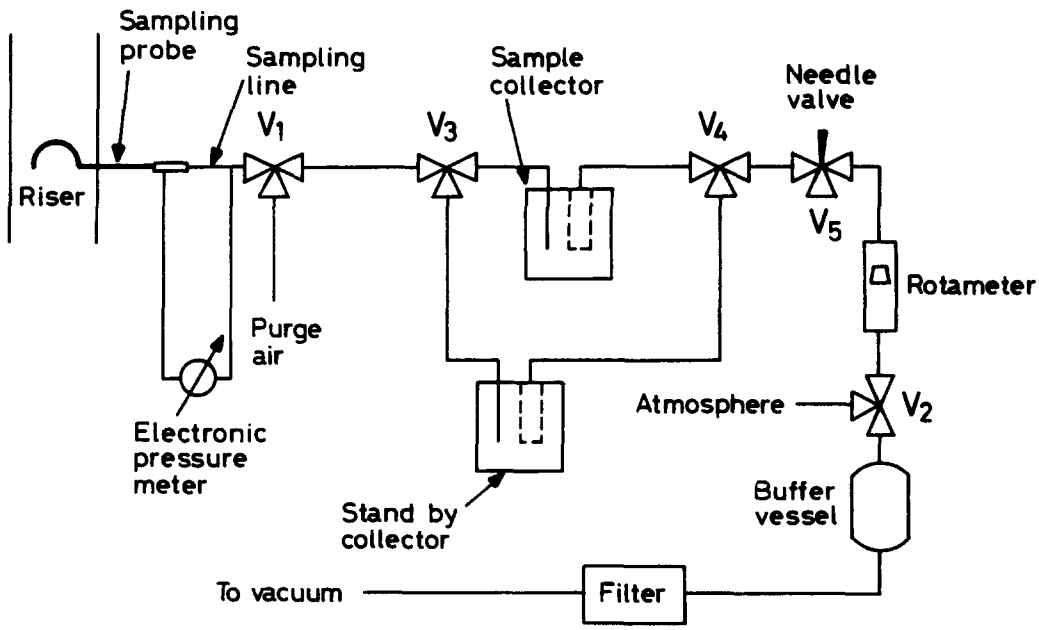

Figure 23. Suction probe and sampling system (Rhodes & Laussmann 1992).

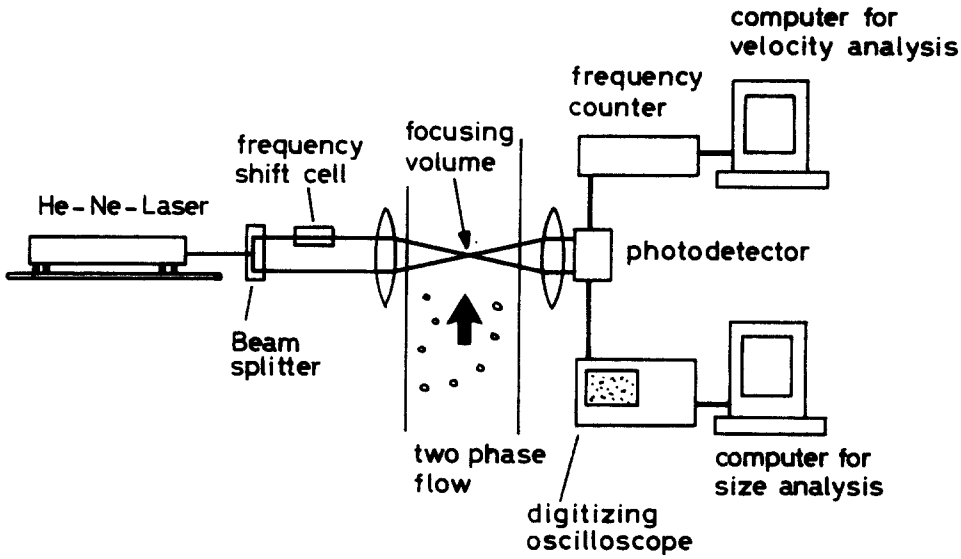

Figure 24. Schematic of the laser-Doppler anemometer system (Arastoopour & Yang 1992).

by a moving particle is subject to a Doppler shift and so by measuring the shift the velocity of the particle may be determined. The equipment used by Arastoopour & Yang (1992) is shown schematically in figure 24. A beam from an He–Ne laser is split into two beams of equal intensity. After passing through a focusing lens, the two beams intersect at the measuring point and generate an interference fringe pattern within the focusing volume, an oval with axes of 184 and 1890 μm. When a moving particle passes through the fringe area the intensity of the scattered light from its surface varies within time to form the "Doppler signal burst" and this is received by the photodetector and processed by the PC software to give a velocity. The technique can also be used to determine particle size. A similar procedure was used by Berkelmann & Reviz (1989) to measure particle and gas velocities in the freeboard region of a bubbling bed.

A novel method which does not require sophisticated data-processing equipment is colour stroboscopic photography, described by Zheng *et al.* (1992). Here the "freezing" effect on moving objects of pulses of light of short duration is used to monitor the motion of fluidized particles. The three basic components of the system are the colour stroboscope, a camera with automatic winder and a microcomputer; the microcomputer synchronizes the stroboscope and the camera in accordance with a predetermined program. Observations were made in a circulating bed riser which contained black particles, which absorb the strobe light, with 3–5% white tracer particles which give coloured images when illuminated. Three flashes of red, blue and yellow light were used for each frame of film recorded and from the resulting coloured images the velocity, acceleration and trajectory of individual particles were obtained.

4. CONCLUSIONS

During the 50 or so years since the widespread introduction of fluidized beds many experimental methods have been devised to study their internal workings. Some of these were prosaic, some ingenious, some were successful, others less so, but with the passage of time the techniques employed have become less invasive, more sophisticated and generally more reliable, particularly when applied to laboratory-scale units. There remains, however, a need for monitoring equipment that can be used reliably on an industrial scale under hostile conditions of atmosphere, temperature and pressure. Some of the probes described above are suited to this type of operation but the question remains about the effect they induce on the local hydrodynamics. Non-invasive techniques, such as radiation attenuation and tomographic imaging, are generally to be preferred but to date these suffer from problems of data interpretation and from the sometimes low level of discrimination they are able to offer. Much remains to be done but, from the range of techniques discussed in this review, it is clear that progress can be made on the basis of firm foundations.

REFERENCES

ARASTOOPOUR, H. & YANG, Y. 1992 Experimental studies on dilute gas and cohesive particles flow behaviour using a laser-Doppler anemometer. In *Fluidization 7* (Edited by POTTER, O. E. & NICKLIN, D. J.). Engineering Foundation, New York.

BARTHOLOMEW, R. N. & CASSAGRANDE, R. M. 1957 Measuring solids concentration in fluidized systems by gamma-ray absorption. *Ind. Engng Chem.* **49,** 428–431.

BAUMGARTEN P. K. & PIGFORD, R. L. 1960 Density fluctuations in fluidized beds. *AIChE Jl* **6,** 115–123.

BERKELMANN, K. G. & REVIZ, U. 1989 The fluid dynamics in the freeboard of an FBC—the use of LDV to determine particle velocity and size. In *Fluidization 6* (Edited by GRACE, J. R, SHEMILT, L. W. & BERGOUGNOU, M. A.). Engineering Foundation, New York.

BLOORE, P. D. & BOTTERILL, J. S. M. 1961 Similarity in behaviour between gas bubbles in liquid and fluidized solid systems. *Nature* **190,** 250–251.

BRACEWELL, R. N. 1986 *The Fourier Transform and its Applications*, 2nd edn. McGraw-Hill, Singapore.

BROADBENT, C. J., BRIDGWATER, J., PARKER, D. J. & HAWKESWORTH, M. R. 1993 Studies of powder mixing in ploughshare mixers using positron emission particle tracking. In *Proc. ECAPT Mtg*, Karlsruhe, Germany, pp. 13–16.

CANADA, G., MCLAUGHLIN, M. H. & STAUB, F. W. 1976 Large particle fluidization and heat transfer at high pressures. *AIChE Symp. Ser.* **75,** 27–37.

CHEREMISINOFF, N. P. 1986 Review of experimental methods for studying the hydrodynamics of gas–solid fluidized beds. *Ind. Engng Chem. Proc. Des. Dev.* **25,** 329–351.

CLOUGH, D. E. & WEIMER, A. W. 1985 Time-dependent behaviour of bubble volume in fluidized beds. *Ind. Engng Chem. Fundam.* **24,** 235–241.

DAVIDSON, J. F. 1961 Discussion following symposium on fluidization. *Trans. Instn Chem. Engrs* **39,** 230–232.

DAVIDSON, J. F. & HARRISON, D. 1963 *Fluidized Particles.* Cambridge University Press, U.K.

DESBAT, L. & TURLIER, P. 1993 Efficient reconstruction with few data in industrial tomography. In *Tomographic Techniques for Process Design and Operation* (Edited by BECK, M. S., CAMPOGRANDE, E., MORRIS, M., WILLIAMS, R. A. & WATERFALL, R. C.), pp. 285–294. Computational Mechanics Publication, Southampton, U.K.

FAN, L. T., HO, T. C., HIRAOKA, S. & WALAWENDER, W. P. 1981 Pressure fluctuations in a fluidized bed. *AIChE Jl* **27,** 388–396.

FAN, L. T., HO, T. C. & WALAWENDER, W. P. 1983 Measurements of the rise velocities of bubbles, slugs and pressure waves in a gas-solid fluidized bed using pressure fluctuation signals. *AIChE Jl* **29,** 33–39.

FOSCOLO, P. U. & GIBILARO, L. G. 1984 A fully predictive criterion for the transition between particulate and aggregate fluidization. *Chem. Engng Sci.* **39,** 1667–1675.

GELDART, D. 1973 Types of gas fluidization. *Powder Technol.* **7,** 285–292.

GELDART, D. 1986 *Gas Fluidization Technology.* Wiley, Chichester, U.K.

GELDART, D. & KELSEY, J. R. 1972 The use of capacitance probes in gas fluidized beds. *Powder Technol.* **6,** 45–60.

GELDART, D. & RHODES, M. J. 1986 From minimum fluidization to pneumatic transport—a critical review of the hydrodynamics. In *Circulating Fluidized Bed Technology*, Vol. 1 (Edited by BASU, P.), pp. 21–31. Pergamon Press, Oxford.

GELDART, D. & XIE, H. Y. 1992 The use of pressure probes in fluidized beds of Group A powder. In *Fluidization 7* (Edited by POTTER, O. E. & NICKLIN, D. J.). Engineering Foundation, New York.

GIBILARO, L. G. 1994 The compressible particle phase hypothesis in fluidization dynamics. Instn Chem. Engrs Research Event, Keynote Lecture.

GIBILARO, L. G., DI FELICE, R., FOSCOLO, P. U. & WALDRAM, S. P. 1988 Fluidization quality: a criterion for indeterminate stability. *Chem. Engng J.* **37,** 25–33.

GUNN, D. J. & AL-DOORI, H. H. 1985 The measurement of bubble flows in fluidized beds by electrical probe. *Int. J. Multiphase Flow* **11,** 535–551.

HAILU, L., PLAKA, F., CLIFT, R. & DAVIDSON, J. F. 1993 Measurement of gas flow through a two-dimensional bubble in a fluidized bed. *Trans. Instn Chem. Engrs* **71,** 382–389.

HALOW, J. S. & NICOLETTI, P. 1992 Observations of fluidized bed coalescence using capacitance imaging. *Powder Technol.* **69,** 255–277.

HARTGE, E. U., LI, Y. & WERTHER, J. 1986 Flow structure in fast fluidized beds. In *Fluidization 5* (Edited by OSTERGAARD, K. & SORENSEN, A.). Engineering Foundation, New York.

HERB, B., DOU, S., TUZLA, K. & CHEN, J. C. 1992 Solid mass fluxes in circulating fluidized beds. *Powder Technol.* **20,** 197–205.

HORIO, M., MONISHITA, K., TACHIBANA, O. & MURATA, N. 1988 Solid distribution and movement in circulating fluidized beds. In *Circulating Fluidized Bed Technology*, Vol. 2 (Edited by BASU, P. & LARGE, J. F.), pp. 147–154. Pergamon Press, Oxford.

HORIO, M., ISHII, H. & NISHIMURO, M. 1992 On the nature of turbulent and fast fluidized beds. *Powder Technol.* **70,** 229–236.

JACKSON, R. 1963a The mechanics of fluidized beds, Part 1. *Trans. Instn Chem. Engrs* **41,** 13–21.

JACKSON, R. 1963b The mechanics of fluidized beds, Part 2. *Trans. Instn Chem. Engrs* **41,** 22–48.

KANG, W. K., SUTHERLAND, J. P. & OSBERG, G. L. 1967 Pressure fluctuations in a fluidized bed with and without screen cylindrical packings. *Ind. Engng Chem. Fundam.* **6,** 499–504.

KECEIOGLU, I., YANG, W-C. & KEAIRNS, D. L. 1984 Fate of solids fed pneumatically through a jet into a fluidized bed. *AIChE Jl* **30,** 1, 99–110.

KEHOE, P. W. K. & DAVIDSON, J. F. 1971 Continuously slugging fluidized beds. *Instn Chem. Engrs Symp. Ser.* **33,** 97–107.

KUNII, D. & LEVENSPIEL, O. 1991 *Fluidization Engineering*. Butterworths, Boston, MA.

LANNEAU, K. P. 1960 Gas–solids contacting in fluidized beds. *Trans. Instn Chem. Engrs* **38,** 125–143.

LEVY, Y. & LOCKWOOD, F. C. 1983 Laser Doppler measurements of flow in the freeboard of a fluidized bed. *AIChE Jl* **29,** 889–895.

LI, Y. & KWAUK, M. 1980 The dynamics of fast fluidization. In *Fluidization* (Edited by GRACE, J. R. & MATSEN, J. M.), pp. 537–544. Plenum Press, New York.

LIN, J. S., CHEN, M. M. & CHAO, B. T. 1985 A novel radioactive particle tracking facility for measurement of solids motion in gas fluidized beds. *AIChE Jl* **31,** 465–472.

LIRAG, R. & LITTMAN, H. 1971 Statistical study of pressure fluctuation in a fluidized bed. *AIChE Symp. Ser.* **67**(116), 11–22.

LITTMAN, H. 1964 Solids mixing in straight and tapered fluidized beds. *AIChE Jl* **10,** 924–929.

LITTMAN, H. & HOMOLKA, G. A. 1970 Bubble rise velocities in two-dimensional gas fluidized beds from pressure measurements. *Chem. Engng Prog. Symp. Ser.* **66,** 37–46.

MARTIN, M. P., TURLIER, P. & BERNARD, J. R. 1992 Gas and solid behaviour in cracking circulating fluidized beds. *Powder Technol.* **70,** 249–258.

MASSIMILLA, L. 1973 Behaviour of catalytic beds of fine particles at high gas velolcities. *AIChE Symp. Ser.* **69,** 11–13.

MERRY, J. M. D. & DAVIDSON, J. F. 1973 "Gulf stream" circulation in shallow fluidized beds. *Trans. Instn Chem. Engrs* **51,** 361–368.

MILITZER, J., HEBB, J. P., JOLLIMORE, G. & SHAKHOURZADEH, K. 1992 Solid particle velocity measurements. In *Fluidization 7* (Edited by POTTER, O. E. & NICKLIN, D. J.), pp. 763–769. Engineering Foundation, New York.

MORSE, R. D. & BALLOU, C. O. 1951 The uniformity of fluidization, its measurement and use. *Chem. Engng Prog.* **47,** 199–211.

MURRAY, J. D. 1965a On the mathematics of fluidization, Part 1. *J. Fluid Mech.* **21,** 465–493.

MURRAY, J. D. 1965b On the mathematics of fluidization, Part 2. *J. Fluid Mech.* **22,** 57–63.

MUSMARRA, D., VACCARO, S., FILLA, M. & MASSIMILLA, L. 1992 Propagation characteristics of pressure disturbances by gas jets in fluidized beds. *Int. J. Multiphase Flow* **18,** 965–976.

NIENOW, A. W. & CHIBA, T. 1985 Fluidization of dissimilar materials. In *Fluidization*, 2nd edn (Edited by DAVIDSON, J. F., CLIFT, R. & HARRISON D.), pp. 357–382. Academic Press, London.

OKHI, K. & SHIRAI, T. 1976 Particle velocity in a fluidized bed. In *Fluidization Technology* (Edited by KEAIRNS, D. L.), pp. 95–119. Hemisphere, New York.

OKHI, K., AKEHATA, T. & SHIRAI, T. 1975 A new method for evaluating the size of moving particles with a fibre optic probe. *Powder Technol.* **11,** 51–57.

ORCUTT, J. C. & CARPENTER, B. H. 1971 Bubble coalescences and the simulation of mass transport and chemical reaction in gas fluidized beds. *Chem. Engng Sci.* **26,** 1049–1064.

ORMISTON, R. M., MITCHELL, F. R. G. & DAVIDSON, J. F. 1965 The velocities of slugs in fluidized beds. *Trans. Instn Chem. Engrs* **43,** 209–216.

PARK, W. H., KANG, W. K., CAPES, C. E. & OSBERG, G. L. 1969 The properties of bubbles in fluidized beds of conducting particles as measured by an electroresistivity probe. *Chem. Engng Sci.* **24,** 851–870.

PARKER, D. J., HAWKESWORTH, M. R., BEYNON, T. D. & BRIDGWATER, J. 1993 Process engineering studies using positron-based imaging techniques. In *Tomographic Techniques for Process Design and Operation* (Edited by BECK, M. S., CAMPOGRANDE, E., MORRIS, M., WILLIAMS, R. A. & WATERFALL, R. C.). Computational Mechanics Publications, Southampton, U.K.

PUT, M., FRANCESCONI, A. & GOOSENS, W. 1973 Determination of the bubble size distribution in gas–solid fluidized beds. In *Proc. Int. Conf. on Fluidization and its Applications*, Toulouse, France, pp. 223–229.

QIN, S. & LIU, G. 1982 Application of optic fibres to measurement and display of fluidized systems. In *Fluidization, Science and Technology* (Edited by KWAUK, M. & KUNII, D.), pp. 258–266. Gordon & Breach, London.

RHODES, M. J. & LAUSSMANN, P. 1992 A simple non-isokinetic sampling probe for dense suspensions. *Powder Technol.* **70,** 141–151.

RHODES, M. J., LAUSSMANN, P., VILLAIN, F. & GELDART, D. 1988 Measurement of radial and axial solids flux variations in the riser of a circulating fluidized bed. In *Circulating Fluidized Bed Technology*, Vol. 2 (Edited by BASU, P. & LARGE, J. F.), pp. 155–164. Pergamon Press, Oxford.

ROWE, P. N. 1971 Experimental properties of bubbles. In *Fluidization*, Chap. 4 (Edited by DAVIDSON, J. F. & HARRISON, D.). Academic Press, London.

ROWE, P. N. & MASSON, H. 1981 Interaction of bubbles with probes in gas fluidized beds. *Trans. Instn Chem. Engrs* **59,** 177–185.

ROWE, P. N. & PARTRIDGE, B. A. 1965 An X-ray study of bubbles in fluidised beds. *Trans. Instn Chem. Engrs* **43,** 157–165.

ROWE, P. N. & YACONO, C. X. R. 1976 The bubbling behaviour of fine powders when fluidised. *Chem. Engng Sci.* **31,** 1179–1192.

ROWE, P. N., PARTRIDGE, B. A., CHENEY, A. G., HENWOOD, G., A. & LYALL, E. 1965 The mechanisms of solids mixing in fluidised beds. *Trans. Instn Chem. Engrs* **43,** T271–286.

ROY, R., DAVIDSON, J. F. & TUPONOGOV, V. G. 1990 The velocity of sound in fluidized beds. *Chem. Engng Sci.* **45,** 3233–3245.

SAXTON, A. L. & WORLEY, A. C. 1970 Modern catalytic-cracking design. *Oil Gas J.* **68,** 82–99.

SEVILLE, J. P. K. 1992 Fluidization of wet particles. In *Proc. 5th Eur. Symp. on Particle Characteristics PARTEC*, Nüremburg, Vol. 2, pp. 801–810.

SEVILLE, J. P. K., MORGAN, J. E. P. & CLIFT, R. 1986 Tomographic determination of the voidage structure of gas fluidised beds in the jet region. In *Fluidization V* (Edited by ØSTERGAARD, K. & SØRENSEN, A.), pp. 87–94. Engineering Foundation, New York.

SIMONS, S. J. R. & WILLIAMS, R. A. 1992 Particle size measurement using non-invasive dielectric sensors. *Powder Technol.* **73,** 85–90.

SIMONS, S. J. R., SEVILLE, J. P. K., BROADBENT, C. J., BRIDGWATER, J., PARKER, D. J., BEYNON, T. D. & HAWKESWORTH, M. R. 1993 The study of particle motion in fluidised beds using positron emission tomography. In *Proc. ECAPT Mtg*, Karlsruhe, Germany, pp. 151–154.

SIMONS, S. J. R., SEVILLE, J. P. K., CLIFT, R., GILBOY, W. B. & HOSSEINI-ASHRAFI, M. E. 1993 Application of gamma-ray tomography to gas fluidised and spouted beds. In *Tomographic Techniques for Process Design and Operation* (Edited by BECK, M. S., CAMPOGRANDE, E., MORRIS, M., WILLIAMS, R. A. & WATERFALL, R. C.), pp. 227–238. Computational Mechanics Publications, Southampton, U.K.

SITNAI, O. 1982 Utilization of the pressure differential records from gas fluidized beds with intervals for bubble parameters determination. *Chem. Engng Sci.* **37,** 1059–1066.

SVOBODA, K., CERMAK, J., HARTMAN, M., DRAHOS, J. & SELUCKY, K. 1983 Pressure fluctuations in gas fluidized beds at elevated temperatures. *Ind. Engng Chem. Proc. Des. Dev.* **22,** 514–520.

SWINEHART, F. M. 1966 A statistical study of local wall pressure fluctuations in a gas fluidized column. Ph.D. Dissertation, Univ. of Michigan, Ann Arbor, MI.

TAYLOR, P. A., LORENZ, M. H. & SWEET, M. R. 1973 Spectral analysis of pressure noise in a fluidized bed. In *Proc. Int. Conf., on Fluidization and its Applications*, Soc. de Chemie Industrielle, Toulouse, pp. 90–98.

TOOMEY, R. D. & JOHNSTONE, H. F. 1952 Gaseous fluidization of solid particles. *Chem. Engng Prog.* **48,** 220–236.

WALLIS, G. B. 1969 *One-dimensional Two-phase Flow*. McGraw-Hill, New York.

WEIMER, A. W., GYURE, D. C. & CLOUGH D. E. 1985 Application of a gamma-radiation density gauge for determining hydrodynamic properties of fluidized beds. *Powder Technol.* **44,** 179–194.

WEINSTEIN, H., FEINDT, H. J., CHEN, L. & GRAFF, R. A. 1992 The measurement of turbulence quantities in a high velocity fluidized bed. In *Fluidization* (Edited by POTTER, O. E. & NICKLIN, D. J.), pp. 305–312. Engineering Foundation, New York.

WERTHER, J. 1993 Fluid mechanics of large-scale CFB units. In *Proc. 4th Int. Conf. on Circulating Fluidized Beds*, Chap. 1. Engineering Foundation, New York.

WERTHER, J. & MOLERUS, O. 1973a The local structure of gas fluidized beds 1. A statistically based measuring system. *Int. J. Multiphase Flow* **1,** 103–122.

WERTHER, J. & MOLERUS, O. 1973b The local structure of gas fluidized beds 2. The spatial distribution of bubbles. *Int. J. Multiphase Flow* **1,** 123–138.

WHITEHEAD, A. B. & YOUNG, A. D. 1967 Fluidization in large scale equipment. In *Proc. Int. Symp. on Fluidization*, pp. 294–302. Netherlands University Press, Amsterdam.

WINTER, O. 1968 Density and pressure fluctuation in gas fluidized beds. *AIChE Jl* **14,** 426–434.

YASUI, G. & JOHANSON, L. N. 1958 Charactedristics of gas pockets in fluidized beds. *AIChE Jl* **4,** 445–452.

YATES, J. G. & CHEESMAN, D. J. 1992 Voidage variations in the regions surrounding a rising bubble in a fluidized bed. *AIChE Symp. Ser.* **88**(289), 34–39.

YATES, J. G., CHEESMAN, D. J. & SERGEEV, Y. A. 1994 Experimental observations of voidage distribution around bubbles in a fluidized bed. *Chem. Engng Sci.* In press.

YERUSHALMI J. & AVIDAN, A. 1985 High-velocity fluidization. In *Fluidization* (Edited by DAVIDSON, J. F., CLIFT, R. & HARRISON, D.), Chap. 7. Academic Press, London.

YOSHIDA, K., NAKAJIMA, K., HAMATAUI, N. & SHIMIZU, F. 1978 Size distribution of bubbles in gas fluidized beds. In *Fluidization* (Edited by DAVIDSON J. F. & KEAIRNS, D. L.), pp. 13–18. Cambridge University Press, U.K.

ZHANG, W., TUNG, Y. & JOHNSSON, F. 1991 *Chem. Engng Sci.* **46,** 3045–3052.

ZHENG, Z., ZHU, J., GRACE, J. R., LIM, C. J. & BRERETON, C. M. H. 1992 Particle motion in circulating and revolving fluidized beds via microcomputer-controlled colour stroboscopic photography. In *Fluidization 7* (Edited by POTTER O. E. & NICKLIN, D. J.). Engineering Foundation, New York.